

Review

## Molybdenum Nitride Films: Crystal Structures, Synthesis, Mechanical, Electrical and Some Other Properties

Isabelle Jauberteau <sup>1,\*</sup>, Annie Bessaudou <sup>2</sup>, Richard Mayet <sup>1</sup>, Julie Cornette <sup>1</sup>,  
Jean Louis Jauberteau <sup>1</sup>, Pierre Carles <sup>1</sup> and Thérèse Merle-Méjean <sup>1</sup>

<sup>1</sup> Université de Limoges, CNRS, ENSCI, SPCTS UMR7315, F-87000 Limoges, France;  
E-Mails: richard.mayet@unilim.fr (R.M.); julie.cornette@unilim.fr (J.C.);  
jean-louis.jauberteau@unilim.fr (J.L.J.); pierre.carles@unilim.fr (P.C.);  
therese.merle@unilim.fr (T.M.-M.)

<sup>2</sup> Université de Limoges, CNRS, XLIM UMR6172, F-87060 Limoges, France;  
E-Mail: annie.bessaudou@unilim.fr

\* Author to whom correspondence should be addressed; E-Mail: isabelle.jauberteau@unilim.fr;  
Tel.: +33-587-502-323; Fax: +33-587-502-304.

Academic Editor: Alessandro Lavacchi

Received: 24 July 2015 / Accepted: 29 September 2015 / Published: 13 October 2015

---

**Abstract:** Among transition metal nitrides, molybdenum nitrides have been much less studied even though their mechanical properties as well as their electrical and catalytic properties make them very attractive for many applications. The  $\delta$ -MoN phase of hexagonal structure is a potential candidate for an ultra-incompressible and hard material and can be compared with c-BN and diamond. The predicted superconducting temperature of the metastable MoN phase of NaCl-B1-type cubic structure is the highest of all refractory carbides and nitrides. The composition of molybdenum nitride films as well as the structures and properties depend on the parameters of the process used to deposit the films. They are also strongly correlated to the electronic structure and chemical bonding. An unusual mixture of metallic, covalent and ionic bonding is found in the stoichiometric compounds.

**Keywords:** molybdenum nitride coatings; film deposition process; crystal structure; mechanical properties; electrical properties; superconductivity

---

## 1. Introduction

Transition metal nitrides as well as carbides are close-packed metallic structures in which nitrogen or carbon atoms occupy the interstitial sites. They can also be viewed as a geometrical arrangement of coordination polyhedra.

Bonding in this structure involves simultaneous contribution of covalent, ionic and metallic bonding to the cohesive energy, which leads to very interesting properties [1,2]. Theoretical as well as experimental works show that metallic bonding is predominant in transition metal nitrides compared with the isostructural carbides [3]. Indeed, the main part of the chemical bonding in carbides is due to  $\sigma$  hybridization of the 2p states of carbon atoms and  $e_g$  components of the d states of metal atoms. The covalent bonding charge between atoms is localized and close to atoms. The contribution of the  $t_{2g}$  component of d states becomes greatly enhanced in the isostructural nitrides and oxides so the metal–metal bond becomes important and the charge in the nitrides is more itinerant and less tightly bound than in the carbides. Moreover, owing to charge transfers from the metal atoms to the nitrogen atoms, an increased ionicity of the chemical bonding is observed in nitrides. These tendencies are confirmed in a recent paper [4]. The calculations of the electronic structure of 4d transition metal mononitrides of NaCl or ZnS-structure types have shown that all mononitrides are metallic. Thus, the different covalency in carbides and nitrides is the main factor responsible for the differences in their mechanical and thermodynamic properties.

These compounds exist over a broad composition range and contain numerous vacancies especially in the nonmetal sites that modify the band structures and thus influence thermodynamic, mechanical, electrical, magnetic and superconducting properties. Because of their extreme hardness, high Young modulus, brittleness and high melting point, they can be considered as ceramic materials. The melting point of TiN equal to 3220 K is higher than the values corresponding to AlN, Al<sub>2</sub>O<sub>3</sub> or Si<sub>3</sub>N<sub>4</sub> equal to 2523, 2323 or 2173 K, respectively. For comparison, the melting point of the Ti parent metal is only equal to 1933 K [2]. They can also be considered as metals since their electronic conductivity is higher than those of ceramic materials. In the same way, the Hall coefficient and the magnetic susceptibility are close to the values of metals. They also have a good chemical resistance. Thus, they can be used in various applications such as hard coatings, corrosion and abrasion resistant layers to protect the tools (few microns thick), or as adaptive tribological coatings with low friction coefficient and wear [5–8] and for micromechanical applications [9]. They are also very interesting as gate electrodes and barriers of diffusion [10–14]. Moreover, their metallic appearance makes them very attractive for decorative coatings. Owing to their electronic structure, transition metal nitrides are also very active in numerous catalytic reactions such as ammonia synthesis or decomposition, CO hydrogenation, NO dissociation and various hydroprocessing [15–21].

Among transition metal nitrides such as Ti, Zr, W, or Cr nitrides, Mo nitrides have been much less studied although they exhibit hardness values ranging from 28 to 34 GPa, whereas those for Ti or Cr nitrides range between 18 and 24 GPa [5,6]. Because of their strong covalent bonding, the calculated values of the bulk modulus of the stoichiometric MoN phase of hexagonal or cubic structure are comparable with those of c-BN and even diamond. Their catalytic activity can be more efficient than more traditional catalysts such as sulfided Ni-Mo/Al<sub>2</sub>O<sub>3</sub> and Co-Mo/Al<sub>2</sub>O<sub>3</sub> [21]. In this work, the passivated  $\beta$ -Mo<sub>2</sub>N<sub>0.78</sub> catalyst displays a high activity at the initial stage of thiofene hydrodesulfurization (HDS)

and its catalytic activity is renewed by a nitriding treatment via temperature programmed reaction (TPR). Mo nitrides are also superconducting and the predicted value of the transition temperature for the metastable MoN phase of NaCl-B1-type cubic structure is the highest of all refractory carbides and nitrides.

Much data about the properties of transition metal carbides and to a lesser extent those of transition metal nitrides has been gathered in some books and reviews [1,2]. Since they have been much less studied, molybdenum nitrides are relatively underrepresented in such works.

This review attempts to fill the gap by collecting relatively recent data about the structure and the formation of molybdenum nitride phases, the method of deposition of films and coatings, their characteristics as well as mechanical, electrical and some other interesting properties.

## 2. Structure of Molybdenum Nitride Phases

### 2.1. $\gamma$ - $\text{Mo}_2\text{N}_{1 \pm x}$ and $\beta$ - $\text{Mo}_2\text{N}_{1 \pm x}$ Phases

Beside the solid solution of nitrogen in molybdenum, the so-called  $\alpha$  phase, which contains 1.08 at % nitrogen, three molybdenum nitride phases are stable in thermal equilibrium according to the binary phase diagram determined by H. Jehn and coworkers [22]. The  $\gamma$ - $\text{Mo}_2\text{N}_{1 \pm x}$  phase is stable at high temperature. Its structure is cubic of NaCl-B1-type and can be described as a face centered cubic array of Mo atoms with N atoms randomly occupying one half of the octahedral interstices of the host metal (Fm3m, space group). Tagliazucca *et al.* [20] have reported another structure for the  $\gamma$ - $\text{Mo}_2\text{N}_{1 \pm x}$  phase, which consists of an ordered array of vacancies (Pm3m, space group) distinguished from the Fm3m space group by the presence of superstructure reflections. Molybdenum nitrides also crystallize in a structure similar to  $\gamma$ - $\text{Mo}_2\text{N}$  with an excess of nitrogen in the lattice and with the formula  $\text{Mo}_3\text{N}_2$  [10].

The  $\beta$ - $\text{Mo}_2\text{N}_{1 \pm x}$  phase is stable at low temperature. Its structure is a face centered tetragonal structure of metal atoms with an ordered array of nitrogen atoms. This structure is often considered as a tetragonal modification of the cubic  $\gamma$ - $\text{Mo}_2\text{N}_{1 \pm x}$  phase with the lattice constant  $c$  doubled (I4<sub>1</sub>/amd, space group) [12,22]. Both phases exist over a wide range of stoichiometry, the transition between them depends on the stoichiometry and lies in the temperature range from 673 to 1123 K. Another tetragonal molybdenum nitride phase has been produced with the formula  $\text{Mo}_{16}\text{N}_7$  [23].

The lattice parameters of both phases are listed in Table 1.

**Table 1.** Lattice parameters of  $\text{Mo}_2\text{N}$  films (<sup>f</sup>) compared with bulk (<sup>b</sup>), and theoretical values (<sup>th</sup>).

Mo–N Phase	Structure	Space Group	Lattice Constants (nm)	References
$\gamma$ - $\text{Mo}_2\text{N}^b$	Face centred cubic	Fm3m	$a = 0.41613$	[24]
			$a = 0.416\text{--}0.419$	[25]
			$a = 0.416$	[26]
			$a = 0.4124$	[27]
			$a = 0.42$	[28]
			$a = 0.4165$	[12]
			$a = 0.4215\text{--}0.4303$	[29]
$\gamma$ - $\text{Mo}_2\text{N}^f$			$a = 0.421\text{--}0.425$	[30]
			$a = 0.419\text{--}0.429$	[31]
			$a = 0.418\text{--}0.429$	[32]

Table 1. Cont.

Mo–N Phase	Structure	Space Group	Lattice Constants (nm)	References
$\beta$ -Mo <sub>2</sub> N <sup>f</sup>	Body centred tetragonal	I4 <sub>1</sub> /amd	$a = 0.416$ $c = 0.800$	[28]
$\beta$ -Mo <sub>2</sub> N <sub>0.85</sub> <sup>f</sup>			$a = 0.4199$ $c = 0.7996$	[33]
$\beta$ -Mo <sub>2</sub> N <sup>f</sup>			$a = 0.4182$ $c = 0.7993$	[34]
$\beta$ -Mo <sub>16</sub> N <sub>7</sub> <sup>b</sup>	Tetragonal		$a = 0.841$ $c = 0.805$	[23]
MoN <sub>0.5</sub> <sup>th</sup>	Cubic		$a = 0.4162$	[35]

## 2.2. Hexagonal $\delta$ -MoN Phase

Only the hexagonal  $\delta$ -MoN phase exists at the stoichiometric composition under thermal equilibrium, and so it can be used as a standard for quantitative spectroscopic analysis. The  $\delta$ -MoN phase crystallizes at least in three different form of the hexagonal structure and one slightly overstoichiometric with composition Mo<sub>5</sub>N<sub>6</sub>. The various forms have been very accurately described in the paper by Ganin *et al.* [36].  $\delta_1$ -MoN has a WC-type crystal structure (P6m2, space group) with stacking faults of nitrogen atoms layers along the c axis due to nitrogen atoms disorder.  $\delta_2$ -MoN crystallizes with the NiAs structure-type (P6<sub>3</sub>/mmc, space group) with an ordered array of nitrogen atoms.  $\delta_3$ -MoN is the much-investigated phase (P6<sub>3</sub>mc, space group), it consists of trigonal Mo clusters and an ordered array of nitrogen atoms so the atomic arrangement can be described as a slightly deformed superstructure of NiAs. The Mo<sub>5</sub>N<sub>6</sub> is the result of an intergrowth structure of the WC and NiAs-type building blocks with vacancies on Mo sites (P6<sub>3</sub>/m or P6<sub>3</sub>22, space group). Molybdenum nitrides also crystallize in Mo<sub>2</sub>N of hexagonal structure [10].

The lattice parameters of the phase are listed in Table 2.

**Table 2.** Lattice parameters of MoN films (<sup>f</sup>) compared with bulk values (<sup>b</sup>), and theoretical values (<sup>th</sup>).

Mo–N Phase	Structure Type	Space Group	Lattice Constants (nm)	References
$\delta$ -MoN <sup>b</sup>	Hexagonal	P6 <sub>3</sub> mc	$a = 0.57402$ $c = 0.56203$	[37]
$\delta$ -MoN <sup>f</sup>	Hexagonal		$a = 0.572$ $c = 0.560$	[25]
			$a = 0.572$ $b = 0.556$	[26]
$\delta_1$ -MoN <sup>f</sup>	Hexagonal WC-type	P6m2	$a = 0.2868$ $c = 0.2810$	[36]
$\delta_3$ -MoN <sup>f</sup>	Hexagonal NiAs-type	P6 <sub>3</sub> mc	$a = 0.57356$ $c = 0.56281$	[36]
Mo <sub>5</sub> N <sub>6</sub> <sup>f</sup>	Hexagonal WC and NiAs-type	P6 <sub>3</sub> /m	$a = 0.48924$ $c = 1.10643$	[36]
MoN <sup>th</sup>	Hexagonal		$a = 0.5787$ $c = 0.5404$	[35]

Table 2. Cont.

Mo–N Phase	Structure Type	Space Group	Lattice Constants (nm)	References
$\delta_1$ -MoN <sup>th</sup>			$a = 0.286$ $c = 0.280$	[38]
$\delta_3$ -MoN <sup>th</sup>			$a = 0.5710$ $c = 0.5625$	[38]
$\delta_1$ -MoN <sup>th</sup>		P6m2	$a = 0.2861$ $c = 0.2843$	[39]
$\delta_2$ -MoN <sup>th</sup>		P6 <sub>3</sub> /mmc	$a = 0.5700$ $c = 0.5661$	[39]
$\delta_3$ -MoN <sup>th</sup>		P6 <sub>3</sub> mc	$a = 0.5721$ $c = 0.5649$	[39]
	Cubic NaCl-B1-type	Fm3m	$a = 0.4212$	[40]
MoN <sup>f</sup>			$a = 0.420$ – $0.427$	[25]
			$a = 0.4215$ – $0.4253$	[41]
			$a = 0.420$ – $0.422$	[26]
MoN <sup>th</sup>			$a = 0.425$	[42]

### 2.3. Metastable Cubic MoN Phase

The stoichiometric MoN phase of NaCl-B1-type cubic structure is thermodynamically unstable. In contrast with  $\gamma$ -Mo<sub>2</sub>N compound, the Fermi level lies well into the antibonding band, which consists primarily of Mo-d- $t_{2g}$  states with a small N-p component. This region of the valence band complex is known to influence the properties of materials such as superconductivity. The transition temperature  $T_c$  of the stoichiometric MoN phase is expected to be high [42] (Section 7.3). Some authors have attempted to stabilize the structure by non-equilibrium techniques such as RF sputtering in high nitrogen partial pressure, nitrogen ion implantation, low energy ion assisted deposition [25,28,41]. Saito *et al.* [26] have reported a continuous transformation of the  $\gamma$ -Mo<sub>2</sub>N phase to the stoichiometric B1-MoN phase by increasing nitrogen incorporation in the structure. The lattice parameter of 0.420–0.422 nm is close to the value equal to 0.425 nm calculated by Papaconstantopoulos *et al.* [42] and to the experimental value of 0.4212 nm reported in the paper of Linker *et al.* [40], which corresponds to the exact stoichiometry.

Savvides [41] found values in the range between 0.4215 and 0.4253 nm depending on the ion energy.

The corresponding lattice parameters of the stoichiometric cubic phase are listed in Table 2 and compared with theoretical values.

### 2.4. Amorphous Structures

Molybdenum nitrides have also been synthesized in the form of amorphous structures such as Mo<sub>72</sub>N<sub>28</sub> [31] and Mo<sub>75</sub>N<sub>25</sub> [9] as well as compounds with N/Mo ratio larger than 1, such as the gold colored Mo<sub>3</sub>N<sub>2</sub> phase [43].

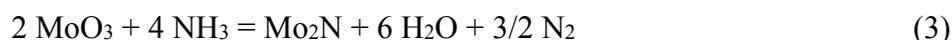
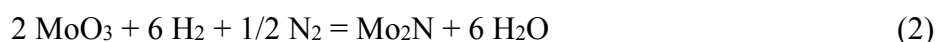
### 3. Formation of Molybdenum Nitride Compounds

#### 3.1. Thermodynamic Analysis

The solubility of nitrogen in molybdenum metal is rather low [22,44]. Direct reactions of the metal with nitrogen gas employ very high temperatures to cleave the strong N–N triple bond. The use of NH<sub>3</sub> instead of N<sub>2</sub> as reactive gas is not easy to control and often leads to a mixture of phases. Moreover, the decomposition of NH<sub>3</sub> is endothermic but it can be replaced by N<sub>2</sub>–H<sub>2</sub> gas mixtures, which circumvent the problem of heat transfer.

In the past years, Lyutaya [45] has developed a thermodynamic analysis of the formation of group VI metal nitrides and especially Mo<sub>2</sub>N.  $\gamma$ -Mo<sub>2</sub>N of face centered cubic structure ( $a = 0.4159$  nm) is prepared from molybdenum powder exposed to an ammonia stream for 8 h at a temperature of 973 K. A molybdenum oxynitride Mo<sub>2</sub>O<sub>1-x</sub>N<sub>x</sub> ( $a = 0.4168$  nm) of face centered cubic structure is synthesized when MoO<sub>3</sub> is exposed to NH<sub>3</sub> at 973 K for 4 h. The author has developed a process to prepare Mo<sub>2</sub>N and MoN by removing oxygen from the molybdenum oxynitride in fast ammonia stream at 1173 K and synthesize Mo<sub>2</sub>N at 973 K for 2 h and MoN at 723 K for a longer period of time.

The author identified three reactions leading to the formation of Mo<sub>2</sub>N:



The isobaric-isothermal potential  $\Delta G^\circ$  is equal to about  $-41.84 \text{ kJ}\cdot\text{mol}^{-1}$  for Reactions (1) and (3) at 500 K but it decreases very strongly with increasing temperature for Reaction (3). The value is slightly lower for Reaction (2). Jehn *et al.* [22] have determined a value of  $-30.38 \text{ kJ}\cdot\text{mol}^{-1}$  for Reaction (1).

#### 3.2. Application to the Synthesis of Molybdenum Nitride Compounds

The reactions previously described occur in the synthesis of molybdenum nitride compounds by temperature programmed reaction (TPR), the so-called ammonolysis from MoO<sub>3</sub> or MoCl<sub>5</sub> precursors in NH<sub>3</sub> gas or N<sub>2</sub>–H<sub>2</sub> gas mixture flow. This method is usually carried out to prepare catalysts. The conditions differ in specific details but all authors apply slow temperature ramp rates and high ammonia space velocities. McKay *et al.* [16,46] have synthesized  $\gamma$ -Mo<sub>2</sub>N from MoO<sub>3</sub> in NH<sub>3</sub> gas at a temperature of 1078 K for 5 h, whereas N<sub>2</sub>–H<sub>2</sub> gas mixture is used to prepare  $\beta$ -Mo<sub>2</sub>N at a temperature of 973 K for 2 h. The authors have reported that  $\gamma$ -Mo<sub>2</sub>N can also be prepared using N<sub>2</sub>–H<sub>2</sub> gas mixture, although much more specific preparation conditions were employed in this synthesis.  $\delta$ -MoN is synthesized in NH<sub>3</sub> gas stream at a temperature of 1078 K for 60 h. The authors have also reported that  $\gamma$ -Mo<sub>2</sub>N decomposes to form  $\beta$ -Mo<sub>2</sub>N and eventually Mo in the ammonolysis of MoO<sub>3</sub> at temperatures greater than 1073 K. It also decomposes to  $\beta$ -Mo<sub>2</sub>N by cooling it in inert gas or heating it to 1273 K in an inert atmosphere.

The formation of molybdenum nitrides proceeds through a set of parallel reactions involving the formation of intermediate compounds. Partially reduced oxides such as MoO<sub>2</sub> or Mo<sub>4</sub>O<sub>11</sub> as well as hydrogen molybdenum bronzes H<sub>x</sub>MoO<sub>3</sub> and molybdenum oxynitrides MoO<sub>x</sub>N<sub>1-x</sub> have been identified

during the reduction nitridation process.  $H_xMoO_3$  exists in four distinct phases in the range  $0 < x \leq 2$  in which hydrogen is inserted into the  $MoO_3$  matrix with small consequential changes in the lattice parameters of  $MoO_3$  [47]. The enthalpy of formation of  $H_xMoO_3$  determined at 298 K is negative for the four phases. The enthalpy of formation of  $MoO_2$  and  $H_2MoO_3$  is equal to  $-598.94$  and  $-80.4$   $kJ \cdot mol^{-1}$ , respectively, compared with the value corresponding to  $MoO_3$ , which is equal to  $-745.05$   $kJ \cdot mol^{-1}$ .

In recent years, Tagliazucca *et al.* [20] studied the properties of molybdenum-based catalysts made from  $MoO_3$  in  $NH_3$  gas flow. The formation of  $H_xMoO_3$  and  $MoO_2$  is observed at a temperature of 613 K during the reduction-nitridation process leading to the synthesis of molybdenum nitrides. Cardenas-Lizana *et al.* [48] have developed a process to produce  $\beta-Mo_2N$  from  $MoO_3$  in  $N_2-H_2$  gas mixture at a temperature of 933 K and observed the reduction of  $MoO_3$  to  $MoO_2$  and Mo. In contrast with many previous studies suggesting that the formation of molybdenum nitride intermediates is a thermochemically controlled process, the authors report a kinetically controlled process.

#### 4. Deposition of Molybdenum Nitride Films and Coatings

Molybdenum nitride films are synthesized by various processes from reactive sputtering to thermal decomposition of precursors.

It is worth noting that in most X-ray diffraction (XRD) studies, it is not easy to differentiate the various phases of molybdenum nitrides, especially  $\gamma-Mo_2N$  and  $\beta-Mo_2N$ . The diffraction patterns show intense reflections close to one another at low Bragg angles. Moreover, the small size of the crystallites results in peaks broadening and owing to the overlapping of peaks arising from molybdenum oxides and molybdenum nitrides, the precise structure of molybdenum nitrides cannot be unambiguously determined. It is well known that crystalline phases in thin films tend to show preferred orientations, so only few diffraction peaks are detected by conventional X-ray diffraction that makes the analysis of the crystal structure difficult. Thus, in the following part, the structure of  $Mo_2N$  phase is only specified when it is unambiguously determined.

##### 4.1. Reactive Sputtering Method

The reactive sputtering of molybdenum target in pure  $N_2$  gas or  $Ar-N_2$  gas mixtures by means of DC (direct current), RF (radio frequency) and magnetron discharges is very often performed in most of works.

Because of the presence of reactive gas, the chemical composition of deposited films is different from the target material. Thus, the stoichiometry of  $MoN$  compounds as well as the crystallization, the structure, and the orientation of crystallites are strongly correlated with nitrogen partial pressure. The lattice parameter values of  $Mo_2N$  produced as thin films are in general higher than the corresponding bulk value equal to 0.41613 nm (Table 1). Moreover, they increase with increasing nitrogen partial pressure. The substrate temperature (external heating or not) plays also a role in the crystallization of films.

Among all reactive sputtering techniques, magnetron sputtering allows large-area deposition, high quality films even at low substrate temperatures. Thus, this technique is widely used in coating processes. Figure 1 shows a schematic representation of a magnetic sputtering system. In this process, a strong magnetic field near the target area is generated which causes the travelling electrons to spiral along magnetic flux lines near the target. Thus, the plasma is confined near the target area that maintains the

stoichiometry and the thickness uniformity of the deposited thin films. The high-density plasma is stable that improves the sputtering process efficiency. Moreover, non-conductive targets can be used and the arcing is reduced because of the use of alternating electric field.

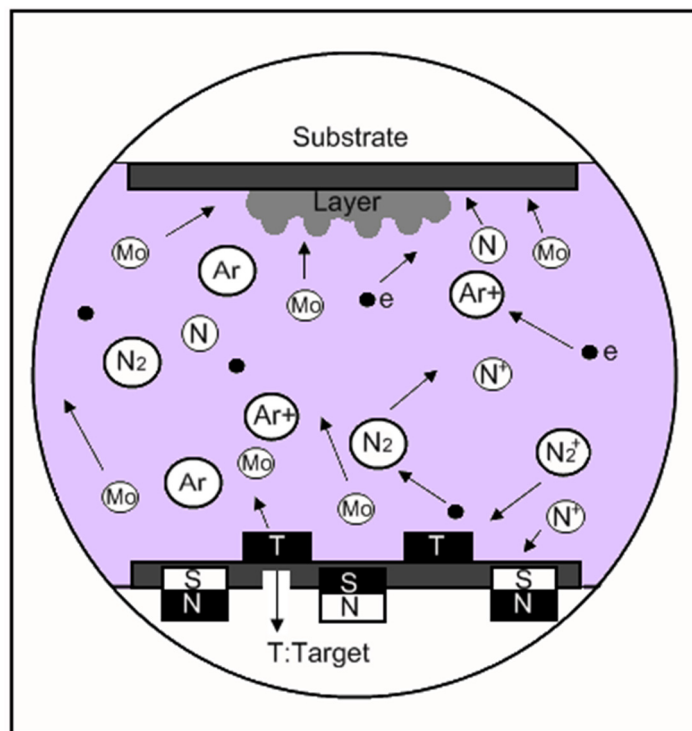


**Figure 1.** Experimental set up of magnetron sputtering method.

#### 4.1.1. Influence of the Nitrogen Pressure on the Formation of Crystalline or Amorphous Mo<sub>2</sub>N Phases

Anitha *et al.* [29] synthesized molybdenum nitride thin films on chemically cleaned glass or silicon substrates by reactive rf magnetron sputtering. The molybdenum target is sputtered in (Ar–N<sub>2</sub>) gas mixtures at nitrogen partial pressures ranging between 1 and  $60 \times 10^{-3}$  Pa. The substrate is heated at temperatures ranging between 300 and 575 K. The authors noticed that the rate of deposition remains relatively constant over a nitrogen partial pressure ranging from 1 to  $20 \times 10^{-3}$  Pa and falls drastically at higher nitrogen partial pressure. The substrate temperature has not any significant effect on the structure as well as on the lattice parameter of the phase, the grain size, and the orientation of crystallites. However, the nitrogen partial pressure exerts a strong influence on the orientation of crystallites since they are randomly oriented at low nitrogen partial pressure ( $4.7$  to  $15 \times 10^{-3}$  Pa). The N/Mo ratio corresponds to the stoichiometric Mo<sub>2</sub>N phase. At larger nitrogen pressure of about  $30$ – $60 \times 10^{-3}$  Pa, the crystallites exhibit strong (200) preferred orientation. In that case the films contain excess nitrogen and hence the lattice parameter increases (Table 1). However, the size of crystallites remains almost constant and equal to 10–25 nm. The morphology of films consists of dense and fibrous crystallites and their surface topography appears to be relatively smooth. This structure is close to the zone T regime of Thornton's structure zone classification [49] with the ratio  $T_s/T_m$  equal to 0.21 where  $T_s$  is the substrate temperature and  $T_m$  the melting temperature (2275 K for Mo<sub>2</sub>N). The growth of molybdenum nitride films occurs under conditions of relatively low adatom mobilities.

The results obtained by Aouadi *et al.* [5] are consistent with the previous ones. The authors synthesized Mo<sub>2</sub>N/MoS<sub>2</sub>/Ag nanocomposites about 2.8 μm thick on hardened 440C grade stainless steels and on inconel 600 substrates from individual targets of Mo, MoS<sub>2</sub> and Ag in (Ar–N<sub>2</sub>) gas mixture with partial pressures of 0.3 and 0.04 Pa, respectively, using an unbalanced magnetron sputtering apparatus. These composite coatings are expected to have tribological properties. The results are consistent with [29] since the Mo<sub>2</sub>N phase is strongly oriented in the (200) crystallographic direction at a nitrogen partial pressure of  $4 \times 10^{-2}$  Pa.

Wang *et al.* [31] have prepared molybdenum nitride films on Si wafers by pulsed dc reactive sputtering. The discharge power is equal to 150 W and the total pressure of (Ar–N<sub>2</sub>) gas mixture is fixed at 0.66 Pa. The films consist of randomly oriented Mo<sub>2</sub>N crystallites at low nitrogen partial pressure about 10%–30% N<sub>2</sub> in (Ar–N<sub>2</sub>) gas mixture ( $6.6$  to  $19.8 \times 10^{-2}$  Pa). Their size decreases with increasing nitrogen partial pressure (29.9 and 17.8 nm at  $6.6$  and  $19.8 \times 10^{-2}$  Pa, respectively). In contrast with [29] the films become amorphous at 50% N<sub>2</sub>. It is worth noting that the nitrogen partial pressure is one order of magnitude larger than in [29]. However, in both works the orientation of crystallites as well as the transition to an amorphous structure seems to be due to an excess of nitrogen in the structure, the N/Mo mole ratio is equal to 0.67 and 0.72 in references [29] and [31], respectively. No columnar structure was observed in all as-deposited films under different nitrogen pressure values [31]. The authors in [31] also investigated the bonding states of nitrogen and molybdenum by using X-ray photoelectron spectroscopy (XPS) and they found a continuous shift of the Mo3d<sub>5/2</sub> XPS peak towards high binding energy from 228.1 eV to 228.5 eV, whereas the N1s XPS peak shifts towards low binding energy with increasing nitrogen partial pressure. This is due to the increase of charge transfer from Mo to N atoms, which leads to a more ionic Mo–N bond.

In a very recent paper, Stöber *et al.* [32] have reported results quite consistent with the previous work. The molybdenum nitride films about 150 nm thick are deposited by reactive dc magnetron sputtering at power ranging from 300 to 700 W and a total pressure ranging from  $2$  to  $8 \times 10^{-1}$  Pa. The crystallites of Mo<sub>2</sub>N are randomly oriented. The films become amorphous at 50% N<sub>2</sub>. Moreover, the authors observe shifts of X-ray diffraction lines, which are explained by the increasing film stress. However, in contrast with [31], the crystallite sizes are much smaller, they range between 3 and 8 nm and the films exhibit a columnar microstructure.

Kattelus *et al.* [9] have developed a deposition process, which allows the directional dependence in intrinsic film stress to be controlled for applications in micromachining. The films are deposited in (Ar–N<sub>2</sub>) gas mixture with an Ar partial pressure of 0.2 Pa using a dc sputtering system. The discharge power is kept constant at 3 kW. In contrast with the previous study [31], the film is amorphous at low nitrogen partial pressure and the first crystalline nitride phase appears at 26% N<sub>2</sub>. It is worth noting that the power used in this work is greatly larger than those used in previous works. The film thickness decreases with increasing nitrogen partial pressure from 300 nm to 200 nm at 26% N<sub>2</sub>.

#### 4.1.2. Influence of the Nitrogen Pressure on the Formation of MoN Phases

Hones *et al.* [30] used the same process as [29] to investigate the structural and mechanical properties of molybdenum nitride films about 1 μm thick in a wide range of nitrogen/metal ratios. The discharge power is kept constant at 120 W, the total pressure of (Ar–N<sub>2</sub>) gas mixture during the sputtering process

is equal to 0.66 Pa and the substrate temperature is fixed at  $500 \pm 20$  K in order to obtain films of structures in the zone T regime of Thornton's structure zone classification which allows optimizing the mechanical properties of films (Section 5). Previous mass spectrometry measurements of plasma species carried on during the sputtering of Cr targets have shown that the plasma consists of positive ions ( $\text{Ar}^+$ ,  $\text{N}^+$ ,  $\text{N}_2^+$ , ...), metallic ions ( $\text{Cr}^+$ ) and compounds ( $\text{CrN}^+$ ). At low nitrogen pressure, the impinging effect of the high flux and kinetic energy of the  $\text{Cr}^+$  ions leads to a densely packed morphology of the films, whereas in absence of a significant amount of high flux and kinetic energy of  $\text{Cr}^+$  ions at higher nitrogen pressure, the films exhibit a columnar morphology. The authors have shown that the nitrogen content in the  $\text{MoN}_y$  films linearly increases with increasing nitrogen partial pressure,  $y$  is the stoichiometric ratio. The randomly oriented crystallites of  $\gamma\text{-Mo}_2\text{N}$  are formed at low nitrogen partial pressure of 0.2 Pa and their size linearly increases from 5 to 18 nm with increasing nitrogen partial pressure up to  $y$  equal to 0.8. A transition from  $\gamma\text{-Mo}_2\text{N}$  of cubic structure to  $\delta\text{-MoN}$  of hexagonal structure occurs at 0.33 Pa and the hexagonal phase becomes predominant at 0.43 Pa. It is worth noting that the nitrogen partial pressure is about one order of magnitude larger than the one reported in [29]. The grain size of the cubic phase decreases with the formation of grains of the hexagonal phase of size equal to 9 nm.

Guntur [12] prepared molybdenum nitride thin films by RF magnetron sputtering in ( $\text{Ar-N}_2$ ) gas mixtures without external heating. The films are deposited under two conditions: at 250 W with a total pressure of 0.93 Pa and at 300 W with a total pressure of 1.6 Pa. The results are consistent with [30] since a transition from  $\gamma\text{-Mo}_2\text{N}$  of cubic structure to  $\text{Mo}_5\text{N}_6$  and then  $\delta\text{-MoN}$  of hexagonal structures is identified at 300 W and nitrogen partial pressures of 0.4 and 0.6 Pa. The same result is obtained at 250 W at nitrogen partial pressures of 0.26 and 0.4 Pa. At larger nitrogen pressure the films become amorphous.

Linker *et al.* [40] and Ihara *et al.* [25] have performed reactive sputtering process with high nitrogen partial pressure to synthesize stoichiometric MoN films of B1-NaCl-type cubic structure because this compound has been predicted to have a higher superconducting transition temperature than NbN (17 K) on the basis of electronic band calculations (Section 7.3). The films 150–400 nm thick have been deposited onto sapphire and glassy carbon substrates in ( $\text{Ar-N}_2$ ) gas mixture at partial pressures of 2.66 and 6.65 Pa, respectively, or in pure nitrogen gas at a pressure of about 20 Pa by using a RF system at a total power of 500 W in [40]. The substrate temperature was varied between room temperature and 1173 K. The stoichiometric MoN films are synthesized at a substrate temperature of 773 K. The resistivity of films has been studied as well as the superconducting temperature (Sections 6 and 7). In [25], the MoN films are prepared by a reactive dc sputtering in pure  $\text{N}_2$  gas at pressures varying between 50 and 140 Pa. The substrate temperature is changed from 673 to 1073 K.  $\text{MoN}_x$  compounds with increasing  $x$  from 0.5 to 1.8 are identified. The authors have investigated the valence band of  $\text{MoN}_x$  films by XPS and they correlated it with the superconducting properties (Section 7.3).

#### 4.2. Reactive Cathodic Arc Evaporation Method

Perry *et al.* [50] have deposited 1.5  $\mu\text{m}$  thick molybdenum nitride films on low carbon steels by means of reactive arc evaporation. The main advantage of this technique is the high degree of ionization of the metal species produced during the evaporation process. The molybdenum is evaporated in ( $\text{Ar-N}_2$ ) at a total pressure of 1.6 Pa with a nitrogen partial pressure ranging between 0.4 and 1.46 Pa. The intensity of arc currents is equal to 130 or 150 A. The substrate is biased to  $-50$  V. The authors investigated the

crystal structure of the as-deposited films very accurately and found that the films synthesized at low nitrogen partial pressures of 0.4 Pa consist of single phase  $\beta$ -Mo<sub>2</sub>N crystallites, whereas single phase  $\delta$ -MoN is formed at 1.4 Pa. The  $\beta$ -Mo<sub>2</sub>N,  $\gamma$ -Mo<sub>2</sub>N and  $\delta$ -MoN phases coexist at pressures ranging between 0.4 and 1.4 Pa. At higher pressure the cubic NaCl-B1-type MoN phase would be synthesized, however, according to the authors it would be rather a metastable nitrogen supersaturated  $\gamma$ -Mo<sub>2</sub>N phase. Its formation could be kinetically controlled.

### 4.3. Ion Implantation Method

#### 4.3.1. Influence of the Temperature on the Formation of Mo<sub>2</sub>N Phases

Mändl *et al.* [28,51,52] have prepared molybdenum nitride coatings by using a plasma immersion ion implantation (PIII) process with high implanted doses of nitrogen ranging between 1.7 and  $3.3 \times 10^{18}$  ions/cm<sup>2</sup> (95% N<sub>2</sub><sup>+</sup>, 5% N<sup>+</sup>) at a pressure of 0.3 Pa. The pure Mo sample of bcc structure and textured with (200) preferred orientation is heated at temperatures up to 1073 K. The results show that  $\gamma$ -Mo<sub>2</sub>N is synthesized at a temperature of 723 K. The film is textured with (200) orientation like the parent metal. However, because of the low size of crystallites resulting in the broadening of diffraction peaks, the formation of the  $\beta$  phase cannot be ruled out. Nevertheless, at temperatures greater than 853 K, a transition from the cubic structure to a tetragonal structure is clearly identified on X-ray diffraction patterns. The authors assigned this transition to the Jahn–Teller effect coupled with a volume reduction by 2.2%.

#### 4.3.2. Influence of Nitrogen Doses on the Formation of Mo<sub>2</sub>N and MoN Phases

Saito *et al.* [26] have synthesized molybdenum nitride films by implanted sputtered Mo thin films with 125 keV N<sub>2</sub><sup>+</sup> ions doses ranging between  $1 \times 10^{17}$  and  $16 \times 10^{17}$  ions/cm<sup>2</sup>. The molybdenum substrate is not heated but the temperature rise is estimated to be about 423 K during the treatment. The authors report that the distribution of implanted nitrogen atoms is not uniform through the films because of the diffusion of nitrogen towards the surface and bulk sides during the treatment. Thus, the nitrogen-implanted thin films probably consist of two phases such as MoN compounds and remaining bcc MoN solid solution. Phase transformations are identified with increasing nitrogen doses:  $\gamma$ -Mo<sub>2</sub>N compound is formed after a dose of  $1 \times 10^{17}$  ions/cm<sup>2</sup>. For a critical dose of  $5 \times 10^{17}$  ions/cm<sup>2</sup>, the lattice parameter strongly increases and becomes close to the predicted value for the stoichiometric MoN of cubic NaCl-B1-type structure (Table 2). The cubic phase coexists with the stoichiometric  $\delta$ -MoN compound of hexagonal structure, which becomes predominant with increasing nitrogen ion doses. The authors have also investigated the chemical bonding states of implanted nitrogen and Mo atoms. The results are consistent with [31] since an electron charge transfer is evidenced. The maximum of the energy shift corresponds to the critical nitrogen dose of  $5 \times 10^{17}$  ions/cm<sup>2</sup>, which results in the formation of the stoichiometric B1-type MoN compound that exhibits the maximum of the superconducting temperature (Section 7.3).

Linker *et al.* [40] have carried out implantation of nitrogen into evaporated Mo films and Mo single-crystal surfaces using multiple ion energies and fluences. They found similar results to those previously described in Section 4.1.2.

#### 4.4. Low-Energy Ion-Assisted Method

Savvides [41] synthesized metastable MoN of B1-type cubic structure 0.4  $\mu\text{m}$  thick by low-energy ion-assisted deposition on fused silica substrates. In this process, the quality of the film is controlled by the energy of ions. It is well known that the ion energy as the relative number of impinging ions to condense atoms arriving at the surface are important parameters affecting the growth morphology, composition, and properties of films. The ion energy ranges from 2 and 200 eV. The presence of chemically active  $\text{N}_2^+$  ions allows the incorporation of nitrogen to be increased, and promotes ordering of the defect structure of cubic MoN. This parameter has a great influence on the value of the superconducting temperature (Section 7.3). The sputtering power is equal to 50 W and the flux of ions impinging on the growing film is equal to  $4 \times 10^{15}$   $\text{cm}^2/\text{s}$ . The substrates are heated at 673, 773 and 973 K. The ion energy greatly influences the film growth as well as the lattice spacing, the superconductivity and the resistivity (Sections 6.2 and 7.3). The grain size distribution remains approximately constant at 24 nm up to 80 eV. The lattice parameter of fcc MoN compounds heated at 773 K is equal to 0.4225 nm at the lowest ion energy, it increases with increasing ion energy and is equal to 0.4253 nm at 100 eV and then decreases to reach the value of 0.4215 nm at 200 eV (Table 2). This is the result of a competition between the increasing concentration of nitrogen in the film and the resputtering of nitrogen by energetic ions. The decrease of the lattice parameter could also be due to the occurrence of compressive stresses arising from argon entrapment. The films deposited at low ion energies up to 100 eV have a strong (200) texture. The texture as well as the size of the grains decrease with increasing ion energy (>100 eV). In general, it is observed a tendency towards ordering in the lattice with increasing ion energy up to 100 eV that is reflected in good electrical properties (Sections 6.2 and 7.3). A slight deterioration in the properties occurs at higher ion energies.

#### 4.5. Pulsed Laser Method

Inumaru *et al.* [33] studied the crystalline structure of the superconducting  $\beta\text{-Mo}_2\text{N}$  phase. The molybdenum nitride films are made on silicon substrates by means of pulsed laser technique with a KrF excimer laser (pulse repetition: 20 Hz) under irradiation of nitrogen radicals with an rf-plasma radical source (power: 350 W). The deposition rate is controlled by changing the power of the laser pulses (energy: 80–300 mJ). Well-crystallized  $\beta\text{-Mo}_2\text{N}$  compound with a moderate orientation in which the c axis is parallel to the Si substrate is identified. The bonding states of nitrogen and molybdenum have also been investigated. The  $\text{Mo}3d_{5/2}$  binding energy of 227.8 eV is close to those of  $\text{Mo}_2\text{C}$  and Mo metal (227.9 eV) and the N1s binding energy equal to 397.5 eV is close to that of the covalent nitride  $\text{Si}_3\text{N}_4$ . Thus, the bond between Mo and N atoms is rather covalent than ionic. The  $\beta\text{-Mo}_2\text{N}$  phase is superconducting at low temperature (Section 7.1).

#### 4.6. Atomic Layer Deposition (ALD)

Alen [11] has made molybdenum nitride films from  $\text{MoCl}_5$  and  $\text{NH}_3$  in a temperature range from 623 to 773 K. The main objective of this study is the deposition of very thin  $\text{MoN}_x$  films about 10 nm thick and the determination of barrier properties. The films are deposited on soda lime and borosilicate glasses

and Si substrates in an ALD reactor operating under a pressure of about 1 kPa. The size of the substrates is equal to  $5 \times 5 \text{ cm}^2$ . Nitrogen gas is used for the transportation of precursors and as a purging gas. The crystal structures vary with temperature. The films consist of  $\gamma\text{-Mo}_2\text{N}$  at 623 K, whereas the films deposited at 673 and 723 K contain both  $\delta\text{-MoN}$  and  $\gamma\text{-Mo}_2\text{N}$  phases and the films deposited at 773 K only consist of  $\delta\text{-MoN}$ . The film growth has been measured as a function of substrate temperature. It increases from 623 to 723 K and then drops from 723 to 773 K (section 6). The author assigned the film growth drop to an etching reaction.

#### 4.7. Plasma Enhanced Chemical Vapor Deposition Techniques

##### 4.7.1. Hexagonal MoN Films

Ganin *et al.* [36] have performed a very accurate study on molybdenum nitride phases of hexagonal structure deposited on wafers of microcrystalline hexagonal boron nitride. The experiments were carried out in a PECVD reactor with  $\text{N}_2$  gas and  $\text{MoCl}_5$  as a precursor at 266 Pa. The deposition occurred in a plasma region inside of a quartz tube between two parallel electrodes (one is connected to a RF source of 13.56 MHz and the other served as a grounded substrate holder). The polycrystalline films about 2  $\mu\text{m}$  thick are black in color. Films of pure  $\delta_1\text{-MoN}$  phase are deposited in the temperature range between 883 and 923 K, whereas  $\delta_3\text{-MoN}$  phase is predominant and identified with  $\delta_2\text{-MoN}$  in films made at higher temperature ranging from 953 to 1003 K. High resolution transmission electron microscopy (HRTEM) as well as selected area electron diffraction (SAED) have been carried out on films. The film of  $\delta_1\text{-MoN}$  consists of mostly disordered crystallites with a typical diameter of 50 nm, whereas the film consisting of  $\delta_3\text{-MoN}$  and  $\delta_2\text{-MoN}$  phases exhibits thin plates, which were mostly perfectly ordered. The authors have reported that  $\text{Mo}_5\text{N}_6$  can be prepared by a reaction of thin Mo films with ammonia at 1023 K. The crystalline structure of all hexagonal MoN phases are described in Section 2.2.

##### 4.7.2. $\beta\text{-Mo}_2\text{N}$ and $\gamma\text{-Mo}_2\text{N}$ Films in Expanding Plasma

Jauberteau *et al.* [34,53–55] have prepared molybdenum nitride films from Mo films coated on Si (100) substrates in an expanding plasma reactor. The molybdenum coatings have been deposited by electron beam evaporation of a molybdenum target in pure Ar atmosphere at a pressure of 0.5 Pa on Si substrates heated at 673 K with a radiofrequency electrical discharge operating at 50 W. The deposition rates are typically equal to 0.02–0.25  $\text{nms}^{-1}$ . The expanding plasma process is very efficient since only 20 min of treatment produces molybdenum nitride thin films about 500 nm thick at low power and even at low temperature. The use of natural gases such as  $\text{N}_2$  without adding any organic precursors allows the process to be performed in the area of compliance with environmental expectations. Moreover, because of the geometry of the expanding plasma, it is expected to process surfaces of dimensions larger than those usually treated and equal to  $1 \text{ cm}^2$ . The substrates are heated at temperatures of 673 or 873 K and exposed to ( $\text{Ar-N}_2\text{-H}_2$ ) gas mixtures at a pressure of 133 Pa. The microwave discharge (2.45 GHz) is produced at a power of 400–500 W in a fused silica tube. The plasma is expanded out of the discharge center into the stainless steel vessel up to the substrate holder.

The conditions of propagation of the electromagnetic wave are satisfied when the density of electrons is above a critical value, which depends on the plasma conditions (collisional or collisionless plasma). The density of electrons is equal to about  $10^{16} \text{ m}^{-3}$  in (Ar–25%N<sub>2</sub>–30%H<sub>2</sub>) gas mixture (the gas contents are expressed as a percentage of the total volume of gas). The authors have shown that the plasma is produced by a surface wave propagating into the reactor along the external surface of the expanding plasma. The reactive species, which are mainly produced on the edge of the plasma, diffuse towards the center of the plasma and react at the surface of the material.

The main objective of this work was to make correlations between the reactive processes occurring in the plasma and on the surface of the material during the formation of metal nitride thin films. The role of hydrogen gas species such as NH<sub>x</sub> or/and H atoms on the formation of molybdenum nitrides has been especially greatly investigated. Since the ion energy at the sheath entrance is low (0.1 eV), the energy of the ion flux, which mainly consists of Ar<sup>+</sup> ions impinging the surface, is too low to produce a sputtering effect on the surface. Thus, the reducing activity on remaining passive layers as oxides is mainly confined to hydrogen species. The β-Mo<sub>2</sub>N phase of tetragonal structure is synthesized in the whole film 400 or 600 nm thick heated at 873 K and exposed to (Ar–25%N<sub>2</sub>–30%H<sub>2</sub>) and (Ar–8%N<sub>2</sub>–10%H<sub>2</sub>) plasma for 20 min. It consists of small columnar grains ranging in size from 20 to 30 nm in the growth direction. The diffusion coefficient of nitrogen ranging between 5 and  $50 \times 10^{-10} \text{ cm}^2\text{s}^{-1}$  is slightly higher than the value assigned to an interstitial atomic diffusion. The N/Mo ratio determined by X-ray photoelectron spectroscopy (XPS) ranges from 0.4 to 0.6. The mean binding energy of 397.45 eV for N1s XPS signal is correlated to the formation of a molybdenum nitride, whereas the Mo 3d<sub>5/2</sub> signal is only slightly higher than the expected one for Mo metallic state. The role of hydrogen species in the plasma has been highlighted by Raman spectroscopy measurements. Hydrogen species such as atomic H, NH<sub>x < 3</sub> radicals in (Ar–N<sub>2</sub>–H<sub>2</sub>) ternary plasma promote the diffusion of nitrogen into the metal film by reducing MoO<sub>2</sub> oxides, which prevent nitrogen from widely diffusing into the film.

In their very recent paper [55], the authors have reported that the crystalline structure of molybdenum nitride films depends on the presence of both remaining oxides in the native molybdenum film and hydrogen species in the plasma. The high temperature γ-Mo<sub>2</sub>N phase is synthesized during a reduction-nitridation process where hydrogen species such as NH<sub>x</sub> (mainly NH<sub>3</sub> molecules and NH<sub>2</sub> radicals) react with the remaining oxides in the metal film. The reaction is exothermic and could involve the formation of intermediates such as hydrogen molybdenum bronze H<sub>x</sub>MoO<sub>3</sub>. Figure 2a shows that the molybdenum film 500 nm thick heated at 873 K and exposed to (Ar–33%N<sub>2</sub>–1%H<sub>2</sub>) plasma for only 30 min mainly consists of strongly oriented γ-Mo<sub>2</sub>N crystallites in the (220) direction. The γ-Mo<sub>2</sub>N/β-Mo<sub>2</sub>N ratio decreases with increasing film thickness (Figure 2b,c). Exothermic reactions occur at the surface of the film during the reduction nitridation process illustrated in Figure 3, which promotes the formation of the high temperature γ-Mo<sub>2</sub>N phase to the detriment of the low temperature β-Mo<sub>2</sub>N phase. The γ-Mo<sub>2</sub>N as well as β-Mo<sub>2</sub>N crystallites exhibit preferred (220) and (204) orientations, respectively, which are probably related to the occurrence of stresses during the growth of films.

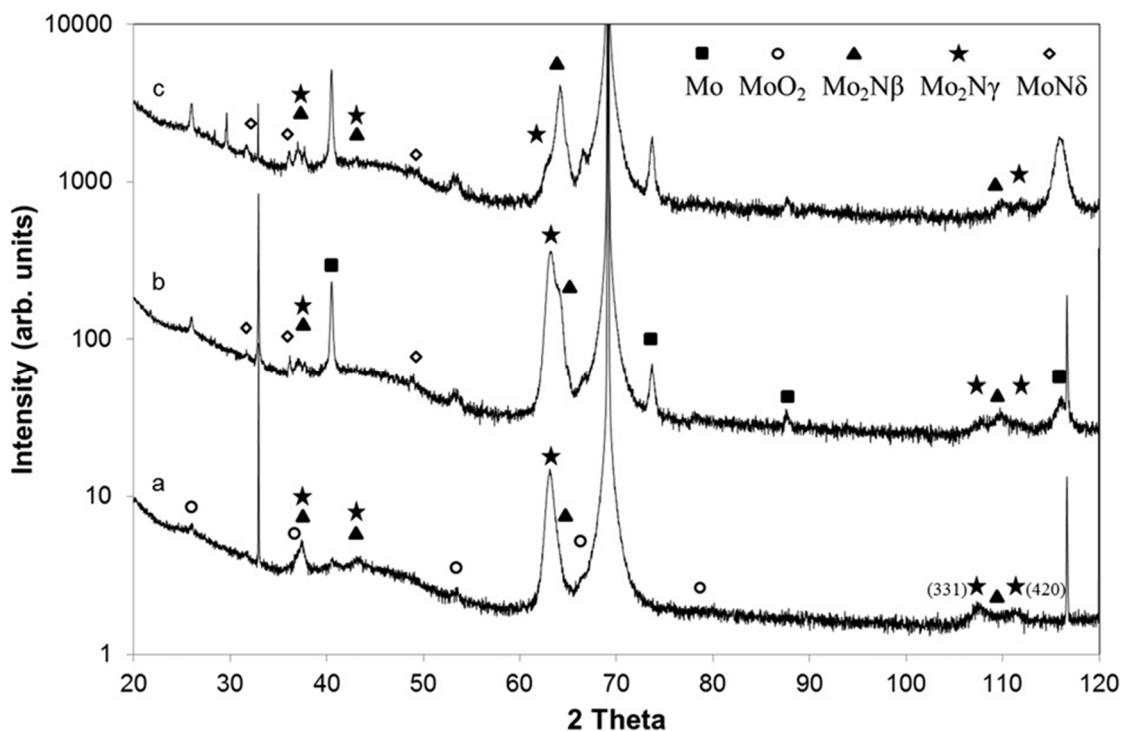


**Figure 2.** (a) X-ray diffraction pattern of molybdenum film 500 nm thick heated at 873 K and exposed to (Ar–33%N<sub>2</sub>–1%H<sub>2</sub>) plasma for 30 min; (b) X-ray diffraction pattern of molybdenum film 800 nm thick heated at 873 K and exposed to (Ar–33%N<sub>2</sub>–1%H<sub>2</sub>) for 1 h; (c) X-ray diffraction pattern of molybdenum film 1 μm thick heated at 873 K and exposed to (Ar–33%N<sub>2</sub>–1%H<sub>2</sub>) for 1 h [55]. Copyright Elsevier 2015.

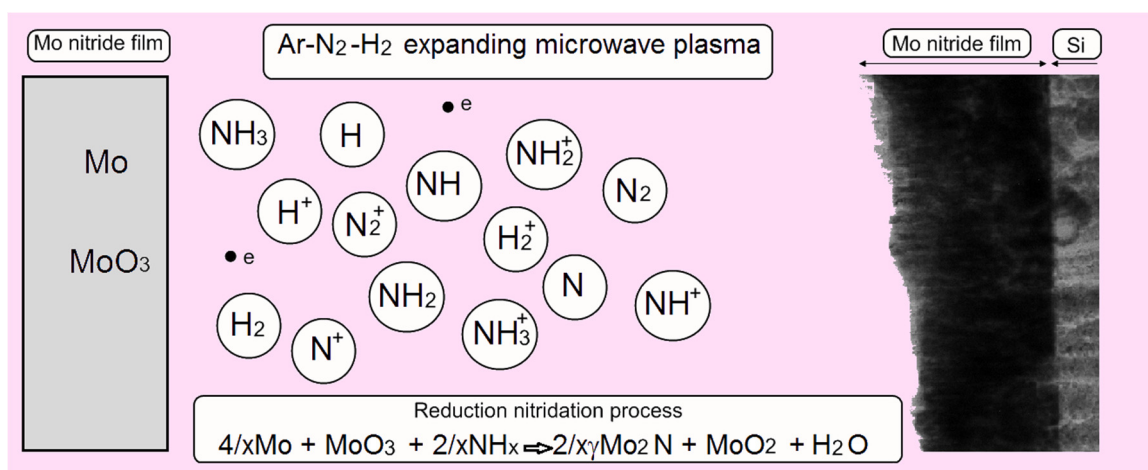


**Figure 3.** Schematic representation of the reduction-nitridation process that occurs during Mo film exposure to (Ar–N<sub>2</sub>–H<sub>2</sub>) expanding microwave plasma.

#### 4.8. Metal Organic Chemical Vapor Deposition

Rische [10] used a metal organic chemical vapor deposition (MOCVD) process to synthesize molybdenum nitride films from two molybdenum guanidinato complexes: the chloro compound Mo(Nt-Bu)<sub>2</sub>Cl [(Ni-Pr)<sub>2</sub>CNMe<sub>2</sub>] and its azido analogue Mo(Nt-Bu)<sub>2</sub>N<sub>3</sub>[(Ni-Pr)<sub>2</sub>CNMe<sub>2</sub>] with and without addition of NH<sub>3</sub>. All experiments are carried out in an horizontal cold wall, glass reactor at

0.1 kPa using nitrogen as carrier gas for 1 h. The process carried out with both chemical complexes used without addition of  $\text{NH}_3$  leads to the formation of molybdenum carbide with only low nitrogen contents. However, when both chemical complexes are used with addition of  $\text{NH}_3$ , the nitrogen content increases up to approximately 30 at % that leads to the formation of  $\gamma\text{-Mo}_2\text{N}$  as dominant phase. The films deposited at temperatures below 773 K are amorphous and those deposited at temperatures between 773 and 1073 K are crystallized. The thickness of films prepared from the chloro compound varies from 200 nm at 673 K to 1300 nm at 1073 K, whereas the one of the film prepared from azido compound varies from 300 nm at 673 K to 1200 nm at 1073 K. The resistivity of films has also been investigated (Section 6).

Fix *et al.* [43] have prepared molybdenum nitride thin films by MOCVD using tetrakis (dimethylamido)molybdenum (IV),  $\text{Mo}(\text{N}(\text{CH}_3)_2)_4$  and ammonia in an atmospheric-pressure laminar flow rectangular glass reactor heated from below. Ultra high purity He gas is used as carrier gas. The results are consistent with those previously reported since all molybdenum nitride films deposited at temperatures ranging from 473 K to 673 K are amorphous. The N/Mo ratio determined by Rutherford backscattering spectroscopy (RBS) is equal to 1.4–1.5. The  $\text{Mo}3d_{5/2}$  and N1s binding energy measured by XPS are equal to 228.4 and 397.3 eV, respectively. The N1s binding energy is close to the values reported for TiN,  $\text{Zr}_3\text{N}_4$ ,  $\text{Ta}_3\text{N}_5$  and other early transition metal nitrides. The H/Mo ratio decreases from 1 to 0.45 with increasing temperature. Because of their amorphous structure, the presence of hydrogen and, so on, the resistivity of films is very high (Section 6).

#### 4.9. Deposition of MoN Coatings by Chemical Process

##### 4.9.1. Polymer Assisted Deposition (PAD)

In a recent paper, Luo *et al.* [56] have reported for the first time the growth of epitaxial molybdenum nitride films with both controlled crystal structures and oxidation states using a chemical solution method. The solution is made from a homogeneous metal polymeric liquid precursors (the polymers are binding with Mo ions) and submitted to a thermolysis and ammonolysis treatment in flowing ammonia. The solution which consists of  $((\text{NH}_4)_6\text{Mo}_7\text{O}_{24}\cdot 4\text{H}_2\text{O})$  is then spin coated on both c-cut  $\text{Al}_2\text{O}_3$  and  $\text{SrTiO}_3$  (001) substrates. This method has produced films with thickness in the range of 35 to 45 nm after one spin-coat. The results showed that  $\delta\text{-MoN}$  of hexagonal structure crystallized on  $\text{Al}_2\text{O}_3$  and  $\gamma\text{-Mo}_2\text{N}$  of cubic structure is synthesized on  $\text{SrTiO}_3$  (001) substrates with a lattice parameter lower than the value corresponding to the bulk  $\gamma\text{-Mo}_2\text{N}$  because of the occurrence of a compressive strain (the lattice parameter of  $\text{SrTiO}_3$  is only equal to 0.39 nm). The lattice parameter of  $\delta\text{-MoN}$  is close to the value corresponding to the bulk value (Tables 1 and 2). Both films are preferentially oriented along the c axis perpendicular to the substrate surface. They are dense and smooth with no detectable microcracks. The root mean square surface roughness is equal to 3–5 nm. Both molybdenum nitride phases are superconducting (Sections 7.1 and 7.2).

##### 4.9.2. Thermal Processes

Maoujoud *et al.* [44] have determined the crystal structures of molybdenum nitride films made by the reaction of ammonia with molybdenum thin films deposited on MgO substrates at temperatures ranging from 573 to 1223 K. The Mo thin films are obtained by thermal evaporation. The film thickness lies

between 60 and 120 nm. The authors have reported that the predominance of one or the other nitride phase is related to the temperature range and the treatment mode. Only  $\gamma$ -Mo<sub>2</sub>N phase is formed at temperatures ranging between 537 and 723 K. However, long treatment times are needed (>15 h), especially at lower temperature limit. The stoichiometric  $\delta$ -MoN phase is synthesized at temperatures ranging between 723 and 1073 K. In contrast with processes previously described, only 2 h of treatment at 998 K are sufficient for a complete transformation. This could be assigned to both nature of the specific surfaces and quantities of starting material.  $\gamma$ -Mo<sub>2</sub>N is also formed in the temperature range 1073–1223 K and only 2 h of treatment at 1098 K is needed.

Nagae *et al.* [57] have prepared molybdenum nitride coatings from a pure molybdenum sheet 1 mm thick prepared by powder metallurgy. The average grain size is equal to 30  $\mu$ m. The nitriding treatment is performed at 1373 K for 16 h in a flowing NH<sub>3</sub> gas at atmospheric pressure. The authors mainly studied the microstructure of molybdenum nitride compounds by transmission electron microscopy (TEM). The surface of the molybdenum nitride sheet consists of  $\gamma$ -Mo<sub>2</sub>N crystallites oriented in the (220) direction, which are randomly oriented at a depth of 25  $\mu$ m. The  $\beta$ -Mo<sub>2</sub>N phase crystallizes from a depth of 35 to 70  $\mu$ m and is rather randomly oriented. The authors have shown that compared with  $\gamma$ -Mo<sub>2</sub>N,  $\beta$ -Mo<sub>2</sub>N consists of lattice defects as twins which are due to stress relaxations.

Khojier *et al.* [8] have synthesized molybdenum nitrides from Mo thin films 100 nm thick deposited on Si substrates in Ar gas at a pressure of 3.2 Pa by d.c. magnetron sputtering operating at 750 V and 125 mA. The Mo thin films are then annealed at temperatures ranging from 673 to 1173 K in flowing nitrogen. The  $\gamma$ -Mo<sub>2</sub>N phase crystallizes at 673 K and the complete transformation of Mo metal in Mo<sub>2</sub>N is achieved at 798 K. Then a cubic-tetragonal transition is identified at a temperature of 1048 K.

Molybdenum nitride coatings are synthesized by conventional thermal equilibrium techniques as well as non-equilibrium methods.

The films are usually 10 nm to 1–2  $\mu$ m thick depending on the process and they are more often deposited on silicon but other substrates can be used such as glass, steel, glassy carbon, sapphire, molybdenum, *etc.* depending on applications. The thickness of films can reach 100  $\mu$ m after a 16 h thermal treatment in NH<sub>3</sub> flow [57]. According to the previously described works, the structure of substrates can be chosen to promote the structure of molybdenum nitrides:  $\delta$ -MoN films/hexagonal BN [36] or  $\delta$ -MoN/Al<sub>2</sub>O<sub>3</sub> and  $\gamma$ -Mo<sub>2</sub>N/SrTiO<sub>3</sub> [56].

Among all non-equilibrium methods, reactive sputtering is very efficient to prepare molybdenum nitride films 1  $\mu$ m thick of various stoichiometry, crystallization, structure (nanocrystalline or amorphous), and with oriented crystallites. The results mainly depend on the nitrogen partial pressure. Among all molybdenum nitride phases,  $\gamma$ -Mo<sub>2</sub>N can be synthesized over a large range of nitrogen pressure from some thousandths of Pascal in (Ar–N<sub>2</sub>) gas mixture [29] to dozens of Pascal in pure N<sub>2</sub> gas [25,40]. Hence, depending on the range of pressure, an increase of pressure leads to contrasting results: A transition from  $\gamma$ -Mo<sub>2</sub>N to stoichiometric MoN phases occurs at large nitrogen partial pressure in (Ar–N<sub>2</sub>) gas mixture [40] or in pure N<sub>2</sub> gas [25,40], whereas transitions from randomly oriented crystallites to oriented crystallites [29] or amorphous structures [31,32] occur at low nitrogen partial pressure. Such phenomena are related to an excess of nitrogen in the lattice and/or the occurrence of stresses during the film growth and so, discrepancies in the values of lattice parameters corresponding to  $\gamma$ -Mo<sub>2</sub>N are clearly seen in Table 1 compared with the bulk and theoretical values.

We can also notice that most works report the formation of  $\gamma$ -Mo<sub>2</sub>N rather than  $\beta$ -Mo<sub>2</sub>N, which are the high and low temperature phases at thermal equilibrium. In our opinion, this is probably because the diffraction patterns corresponding to both phases are not easy to differentiate by conventional X-ray diffraction measurements for the reasons previously evoked. The  $\beta$ -Mo<sub>2</sub>N crystallization has been reported by means of a diffractometer equipped with a multi-axes sample stage [33].

In other non-equilibrium processes such as nitrogen implantation, both nitrogen doses and temperature play a role. In [28], a transition from  $\gamma$ -Mo<sub>2</sub>N to  $\beta$ -Mo<sub>2</sub>N occurs at high temperature and in [26], transitions from  $\gamma$ -Mo<sub>2</sub>N to stoichiometric MoN compounds occur at high nitrogen doses. However, a similar transition is identified at high temperature during the thermal treatment of molybdenum films in flowing nitrogen [8] although this process cannot be compared with reactive sputtering or ion implantation processes. This effect is related to an increase of grain size at high temperature, which deteriorates the mechanical properties. The formation of both high temperature  $\gamma$ -Mo<sub>2</sub>N phase and low temperature  $\beta$ -Mo<sub>2</sub>N phase in expanding plasma is also rather unexpected since it is a non-equilibrium process because the temperature of electrons is much larger than the temperature of heavy species [55]. The authors assumed that exothermic reactions occur at the surface of the substrate between hydrogen species produced in the plasma and the remaining oxides in the molybdenum film, which promote the formation of the high temperature  $\gamma$ -Mo<sub>2</sub>N phase.

Among all molybdenum nitride phases, the stoichiometric metastable B1-MoN can be only obtained by non-equilibrium growth techniques such as reactive sputtering, ion implantation, *etc.* However, oxygen contamination, nitrogen vacancies, other defects and radiation damage in the compounds synthesized by reactive sputtering and ion implantation prevent the predicted structure with high superconducting temperature from forming. It is worth noting that the lattice parameters corresponding to B1-MoN listed in Table 2 are equal to the theoretical value [42] when they correspond to overstoichiometric phase as for example MoN<sub>1.8</sub> [25]. Thus, the excess of nitrogen in the lattice would allow the predicted structure to be achieved. However, as we will see in Section 7, the excess of nitrogen in the structure decreases the superconducting temperature.

## 5. Mechanical Properties of Molybdenum Nitride Coatings

Hardness, compressibility, elastic modulus, and residual stress are significant properties of hard coatings. It is worth noting that generally high compressive stresses lead to harder films, whereas tensile stresses lead to softer films. Alloying molybdenum with nitrogen makes the nitride harder than the pure metal. Thus, the molybdenum nitride phases are less compressible than the parent pure metal. In fact the hardness, bulk modulus as well as Young's modulus resemble those of ceramics. Covalent bonds lead to high bulk modulus and sometimes large mechanical hardness.

### 5.1. $\gamma$ -Mo<sub>2</sub>N Phase

The hardness of  $\gamma$ -Mo<sub>2</sub>N phase is higher than those of transition metal nitrides such as ZrN, VN, NbN, HfN and TaN. It is equal to the value corresponding to Si<sub>3</sub>N<sub>4</sub>. Moreover, its compressibility is low. The bulk modulus of  $\gamma$ -Mo<sub>2</sub>N has been determined by high pressure-high temperature method [24], it is equal to 304 GPa (Table 3).

**Table 3.** Bulk modulus, Young's modulus and hardness of Mo<sub>2</sub>N and MoN films (<sup>f</sup>) compared with bulk values (<sup>b</sup>), and theoretical values (<sup>th</sup>). The thickness (if known) is indicated in brackets. The values for Mo, cBN and C (diamond) are also indicated.

Mo–N Phase Thickness (μm)	Bulk Modulus (GPa)	Young's Modulus (GPa)	Hardness (GPa)	References
Mo	264.7	320	1.53	[2,38,39]
γ-Mo <sub>2</sub> N <sup>b</sup>	304		16	[2] [24]
γ-Mo <sub>1.8</sub> N <sup>f</sup> (1)		365	28–29	[30]
γ-Mo <sub>2</sub> N <sup>f</sup> (0.1)		210	12	[8]
β-Mo <sub>2</sub> N <sup>f</sup> (0.1)		130	6–7	[8]
cubic MoN <sub>0.5</sub> <sup>th</sup>	348			[35]
δ <sub>3</sub> -MoN <sup>b</sup>	345			[58]
δ-MoN <sub>1.2</sub> <sup>f</sup> (1)		420	26–27	[30]
hex MoN <sup>th</sup>	392			[35]
δ <sub>3</sub> -MoN <sup>th</sup>	338–351			[59]
δ <sub>1</sub> -MoN <sup>th</sup>	377	640		[38]
δ <sub>3</sub> -MoN <sup>th</sup>	379	611		[38]
	327	534	29	[39]
δ <sub>2</sub> -MoN <sup>th</sup>	356	600	34	[39]
δ <sub>1</sub> -MoN <sup>th</sup>	353	463		[39]
cubic MoN <sup>th</sup>	389			[35]
cubic MoN <sup>b</sup>	390			[60]
cubic MoN <sup>th</sup>	352	462		[38]
cubic BN <sup>b</sup>	370		60	[24]
C (diamond) <sup>b</sup>	443	900	110	[2]

Hones *et al.* [30] studied the mechanical properties of 1 μm thick molybdenum nitride films MoN<sub>y</sub> made by RF reactive magnetron sputtering (Section 4.1.2). The nitrogen stoichiometry *y* increases with increasing nitrogen partial pressure. The hardness has been measured by nanoindentation at 150–200 nm depth to avoid influence of the surface roughness and substrate. The hardness of γ-Mo<sub>2</sub>N lies at 29 GPa. However, the value decreases with increasing nitrogen content (from *y* = 0.4 to 0.8). The elastic modulus qualitatively follows the evolution of the hardness (Table 3). This behavior is correlated to the change in the electronic structure. The electron concentration increases with increasing *y* that leads to the filling of antibonding electronic states and then the cohesive energy decreases. The cubic phase exhibits tensile stresses, which increase up to 2 GPa with increasing *y*.

In contrast, Kattelus *et al.* [9] have reported compressive effective stresses in Mo–N films from 200 to 300 nm thick deposited by d.c. reactive sputtering for all compositions and structures of films from amorphous state (13%–17% N<sub>2</sub>) to crystalline phase (26% N<sub>2</sub>) (Section 4.1.1). However, the effective stress value for amorphous state can be tailored from compressive through zero into tensile by adding further argon gas into the deposition chamber.

Stöber *et al.* [32] have shown that a minimum film stress of –60 MPa is measured in Mo<sub>2</sub>N films produced with N<sub>2</sub> fraction in (Ar–N<sub>2</sub>) gas mixture of 20% in a reactive dc magnetron sputtering process. The compressive stress increases with increasing nitrogen fraction up to a value of –4 GPa, which leads

to adhesion problems and delamination due to an excess of nitrogen in the structure. The authors noticed an increase of the compressive stress with increasing plasma power values, whereas the increase of gas pressure leads to decreasing stress levels. This behavior is assumed to be correlated to the energy of the particles impinging the surface.

The mechanical properties of films are correlated to the grain size, film density and stoichiometry as well as to crystallographic orientations. A close-packed structure with small crystallites results in higher hardness.

Khojier *et al.* [8] have investigated the mechanical properties of molybdenum films, only 100 nm thick subsequently annealed in flowing N<sub>2</sub> (Section 4.9.2). The hardness and the bulk modulus of thin films have been measured *versus* annealing temperature. The hardness and the bulk modulus increase from 4 to 12 GPa and from 120 to 210 GPa, respectively, with increasing temperature from 673 to 923 K, which corresponds to the transformation of pure Mo of bcc structure to  $\gamma$ -Mo<sub>2</sub>N of fcc structure. Then a further increase of the annealing temperature results in a strong decrease of both parameters because of the formation of the Mo<sub>2</sub>N phase of tetragonal structure at 1048 K with larger grain size. They are equal to 6–7 GPa and 130 GPa, respectively (Table 3).

Lowther *et al.* [35] have performed *ab initio* electronic structure calculations to determine the bulk modulus of the nonstoichiometric MoN<sub>0.5</sub> phase of cubic structure. The value is equal to 348 GPa (Table 3).

## 5.2. Stoichiometric $\delta$ -MoN and Cubic MoN Phases

The bulk modulus values corresponding to stoichiometric MoN compounds of hexagonal and cubic structure are very high. They are found in the range of compressibility of diamond (Table 3).

Hart *et al.* [60] have reported that although nitrides of Zr, Nb and Mo have very similar density of states (DOS), the DOS at the Fermi level increases with increasing number of valence electrons, *i.e.*, from Zr to Mo. In the same way the lattice constant decreases, whereas the bulk modulus increases with increasing number of valence electrons.

According to Soignard *et al.* [58], the stoichiometric hexagonal  $\delta$ -MoN phase is a potential candidate for an ultra-incompressible and hard material since the authors determined a value of 345 GPa for the bulk modulus of  $\delta_3$ -MoN (P6<sub>3</sub>mc, space group).

The hardness of  $\delta$ -MoN is similar to the one measured for  $\gamma$ -Mo<sub>2</sub>N [30], whereas the elastic modulus is somewhat higher (Table 3). In contrast with  $\gamma$ -Mo<sub>2</sub>N, compressive stresses are measured for the hexagonal phase.

Sahu *et al.* [59] have calculated the bulk modulus corresponding to the  $\delta_3$ -MoN phase using the density functional theory. The value agrees with the experimental value of 345 GPa [58]. The authors report that the Mo–N bonding has a small covalent but large ionic component.

*Ab initio* electronic structure calculations [35] have given bulk modulus values of 392 and 389 GPa for the hexagonal and cubic structure of MoN, respectively. For comparison the bulk modulus of diamond is equal to 443 GPa.

Kanoun *et al.* [38] and more recently Zhao *et al.* [39] have also calculated the bulk modulus corresponding to the stoichiometric MoN phase of hexagonal structure by use of the density functional theory (Table 3). The analysis of the density of states of  $\delta_1$ -MoN and  $\delta_3$ -MoN phases show that the high values of bulk modulus result from the covalent character of the bonding due to the strong hybridization

between N and Mo states [38]. The authors have also observed a strong directional charge redistribution from Mo to N atoms, which reflects the electronegative nature of N atoms and adds an ionic contribution to the metallic character of compounds. The authors have concluded that  $\delta_1$ -MoN and  $\delta_3$ -MoN phases exhibit an unusual mixture of metallic, covalent and ionic bonding.

Zhao *et al.* [39] have reported that among the hexagonal structures,  $\delta_2$ -MoN has the largest bulk modulus, which is equal to 356 GPa. This value can be compared with the one of c-BN equal to 370 GPa. This compound also exhibits the largest shear modulus, Young's modulus, and the smallest Poisson's ratio equal to 246 GPa, 600 GPa, and 0.22, respectively, that makes  $\delta_2$ -MoN an intrinsically strong solid and so a potential candidate for an ultra-incompressible and hard material.

As far as MoN phase of cubic structure is concerned and according to Hart *et al.* [60], the experimental instability of the phase could be explained by a negative  $C_{44}$  elastic constant. Moreover, the application of hydrostatic pressure on the structure seems to enhance the instability.

In summary, the analysis of Table 3 shows the dependence of mechanical properties with parameters such as grain size, lattice parameters, *etc.* The highest value of the hardness has been observed for  $\gamma$ -Mo<sub>2</sub>N 1  $\mu\text{m}$  thick and  $\delta_2$ -,  $\delta_3$ -MoN. Such values are explained by the morphology of compounds and are linked with their electronic structures. An excess of nitrogen in coatings leads to compressive stresses and then to adhesion problems.

## 6. Resistivity

The resistivity of molybdenum nitride films has been widely investigated in numerous works. The values greatly depend on the structure, crystal orientation, nitrogen concentration, and so on. The values are higher than the bulk one of 19.8  $\mu\Omega\text{cm}$  (Table 4). They range between 100  $\mu\Omega\text{cm}$  for MoN<sub>x</sub> films 10 nm thick consisting of  $\delta$ -MoN of hexagonal structure and made by atomic layer deposition (ALD) [11] and  $10 \times 10^3 \mu\Omega\text{cm}$  for amorphous Mo<sub>2</sub>N<sub>3</sub> films prepared by metal organic chemical vapor deposition (MOCVD) at low temperature and atmospheric pressure [43] (Sections 4.6 and 4.8). Such a high value is probably due to high nitrogen content, small grain size, amorphous structure and/or large hydrogen content. Figure 4 illustrates the change of deposition rates and resistivity of MoN<sub>x</sub> films *versus* deposition temperature [11]. The drop of the deposition rate is assumed to be due to an etching reaction.

**Table 4.** Resistivity and superconducting temperature of Mo<sub>2</sub>N and MoN films (<sup>f</sup>) compared with bulk values (<sup>b</sup>), theoretical values (<sup>th</sup>), Mo, and C (diamond). The amorphous structures are indicated with (a). The thickness of films (if known) is indicated in brackets.

Mo–N Phase Thickness ( $\mu\text{m}$ )	Resistivity ( $\mu\Omega\text{cm}$ )	$T_c$ (K)	References
Mo <sup>b</sup>	5.47		[2]
Mo <sup>f</sup>	7.5–12		[31]
Mo <sup>f</sup> (0.3)	13		[9]
Mo <sub>2</sub> N <sup>b</sup>	19.8		[2]
$\gamma$ -Mo <sub>2</sub> N <sup>b</sup>		5.2	[24]
Cubic Mo <sub>2</sub> N <sup>f</sup>		6–7	[25]
$\gamma$ -Mo <sub>2</sub> N <sup>f</sup> (0.15)	25–80	4–6	[26]
Mo <sub>2</sub> N <sup>f</sup> (0.2)	180		[9]

Table 4. Cont.

Mo–N Phase Thickness ( $\mu\text{m}$ )	Resistivity ( $\mu\Omega\text{cm}$ )	$T_c$ (K)	References
$\text{Mo}_2\text{N}^f$	500–900		[29]
	300–550		[31]
$\gamma\text{-Mo}_2\text{N}^f(0.01)$	100		[11]
$\gamma\text{-Mo}_2\text{N}^f(1)$	2483		[10]
$\gamma\text{-Mo}_2\text{N}^f$	245		[12]
		4.5	[56]
$\text{Mo}_2\text{N}^f$	150–460		[32]
$\beta\text{-Mo}_2\text{N}^f(0.036)$		5.2	[33]
(a) $\text{Mo-N}^f$	1250		[31]
(a) $\text{Mo}_2\text{N}_3^f$	$10^4$		[43]
$\delta\text{-MoN}^f(0.15)$	110	4	[26]
$\delta_1\text{-MoN}^f$		4	[36]
$\delta_3\text{-MoN}^f$		12	[36]
$\text{Mo}_5\text{N}_6^b$		12	[36]
	1000		[12]
$\delta\text{-MoN}^f$		12	[56]
		13.2	[25]
cubic $\text{MoN}^f(0.15\text{--}0.4)$	850–1700	3–6	[40]
cubic $\text{MoN}^f$	40–70	6.8	[26]
cubic $\text{MoN}^f(0.4)$	120–200	5–6.15	[41]
cubic $\text{MoN}^{\text{th}}$		29.4	[42]
C (diamond) <sup>b</sup>	$10^{18}$		[2]

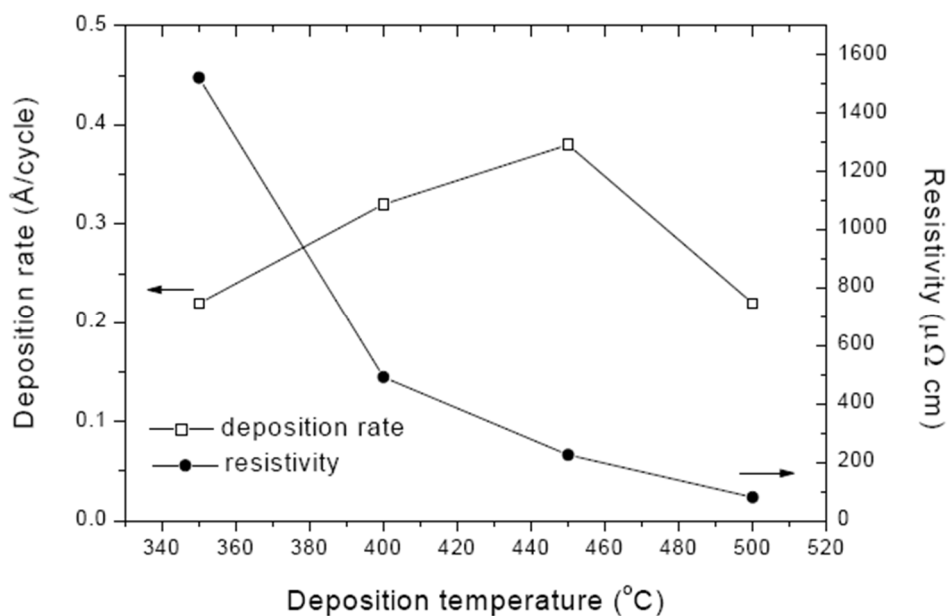


**Figure 4.** Deposition rates and resistivities of  $\text{MoN}_x$  films as a function of deposition temperature (according to Alen, Ph.D. thesis, 2005 [11]).

### 6.1. Molybdenum Nitride Films Prepared by Reactive Sputtering

The resistivity of films made by reactive sputtering increases with increasing nitrogen partial pressure. This is due to the increasing amount of nitrogen atoms in the lattice. Compared with pure molybdenum films, the high resistivity values of MoN<sub>x</sub> films might be attributed to the scattering of electrons because of small grain size, and thus populated grain boundaries as well as distorted structures in films deposited at high nitrogen partial pressure.

According to Anitha *et al.* [29], the resistivity depends strongly on the size and the preferred orientation of crystallites. The films with large grain size and strong orientation exhibit local minima in the resistivity *versus* nitrogen partial pressure curves.

Moreover, the temperature dependence of resistivity for all films investigated in the temperature range 30–300 K exhibits a negative coefficient of resistivity.

The measured resistivity  $\rho$  is written:

$$\rho = \rho_0 + \rho(t) \quad (4)$$

where  $\rho_0$  is the residual resistivity due to the electron scattering by defects, it corresponds to the compositional, topological and structural disorder in the sample and  $\rho(t)$  is the temperature dependent contribution due to the electron–phonon interaction.

According to the authors, the negative temperature coefficient is probably due to grain-boundary related effects and the presence of oxygen impurity in the films.

As a general rule, the resistivity strongly decreases at high annealing temperatures because of the increase in film crystallinity and removal of structural distortions, which result in enhanced phonon scattering of electrons.

In the paper by Wang *et al.* [31], the sheet resistivity increases with increasing nitrogen partial pressure from 300 to 1250  $\mu\Omega\text{cm}$ , which corresponds to Mo<sub>2</sub>N crystallized compounds and amorphous structures, respectively. The value of 1250  $\mu\Omega\text{cm}$  drastically drops to 650  $\mu\Omega\text{cm}$  after 1073 K annealing that corresponds to the formation of Mo<sub>2</sub>N crystallites.

Kattelus *et al.* [9], who observed a transition from amorphous to crystallized structures (Section 4.1.1), report a resistivity of 180  $\mu\Omega\text{cm}$  for crystallized Mo<sub>2</sub>N films 200 nm thick.

In his Ph.D. works, Guntur [12] have reported that the increase of the resistivity values of molybdenum nitride films with increasing nitrogen partial pressure is due to the transition from cubic Mo<sub>2</sub>N structure to hexagonal MoN structure (Table 4).

Stöber *et al.* [32] have also reported an increase of the resistivity of Mo<sub>2</sub>N films with increasing nitrogen fraction in (Ar–N<sub>2</sub>) gas mixtures. The resistivity of Mo<sub>2</sub>N films deposited at 20% of nitrogen fraction, a pressure of 500 W and a total pressure of  $8 \times 10^{-1}$  Pa is equal to 200  $\mu\Omega\text{cm}$ . The authors have especially noticed that the temperature coefficient of resistance (TCR) changes from positive to negative *versus* temperature. For nitrogen fraction ranging from 5% to 20%, a transition from a thermally activated charge transfer mechanism over the grain boundary (TCR < 0) to a thermally activated charge transfer by means of electron–phonon interaction (TCR > 0) at 473 K occurs. For a nitrogen fraction larger than 30%, the films exhibit a semi-conductor like behavior.

The values determined by Linker *et al.* [40] range between 850 and 1700  $\mu\Omega\text{cm}$  for the stoichiometric MoN films. It is worth noting that ion irradiation induces various kinds of lattice defects and hence

deteriorates the related physical properties. The authors have also determined the residual resistivity ratio  $\rho(300\text{ K})/\rho(4.2\text{ K})$  that is indicative of disorder in MoN. They found values ranging between 1 and 0.8. The value decreases dramatically for overstoichiometric MoN<sub>x</sub> films ( $x > 1$ ). At  $x = 1.8$ , the residual resistivity  $\rho(25\text{ K})$  is very high and equal to 2.2  $\Omega\text{cm}$  which might be due to the columnar structure of films.

### 6.2. Molybdenum Nitride Films Prepared by Low-Energy Ion-Assisted Process

Savvides [41] have reported a very detailed study on the influence of ion energy on the structure and resistivity of molybdenum nitride films (Section 4.4). The MoN films deposited at 773 K at ion energy range 2–130 eV exhibit high resistivity values characterized by a negative temperature coefficient, which corresponds to disordered crystalline and amorphous metals.

In fact, the defect-dependent residual resistivity dominates the measured resistivity. Thus, the temperature-dependent contribution is weak and anomalous, pointing to anomalous electron transport, which can be understood in terms of disorder and localization. For ion energy above 130 eV, there is a transition in properties to those of a more ordered material. The temperature coefficient of resistivity is positive but the temperature-dependent contribution is still weak and anomalous. The transition occurs at about 150  $\mu\Omega\text{cm}$  and coincides with Mott's minimum metallic conductivity. However, at high flux of high-energy ions, a competition takes place with ion-induced structural disorder and loss of nitrogen.

The temperature coefficient of resistivity strongly increases when the films are subsequently annealed at 973 K after ion sputtering at 773 K. The MoN films exhibit metallic behavior. Moreover, the temperature dependence of the thermal contribution of annealed samples exhibits a  $T^2$  relation, which is observed for high  $T_c$  superconductors instead of the classical  $T^n$  ( $n = 3\text{--}5$ ) dependence usually seen in simple metals and low  $T_c$  superconductors.

### 6.3. Molybdenum Nitride Films Prepared by Ion Implantation

In the paper by Saito *et al.* [26], the resistivity increases almost linearly with increasing nitrogen dose. The results are both ascribed to the transition from cubic  $\gamma\text{-Mo}_2\text{N}$  to NaCl-B1-type MoN and the formation of hexagonal  $\delta\text{-MoN}$ . Compared with Linker *et al.* results, the residual resistivity ratio slightly decreases with increasing nitrogen dose and the resistivity of films ranges between 25 and 110  $\mu\Omega\text{cm}$  (Table 4).

In summary, the highest values of resistivity have been reported for  $\gamma\text{-Mo}_2\text{N}$  1  $\mu\text{m}$  thick, amorphous MoN (10,000  $\mu\Omega\text{cm}$ ) and cubic MoN films. The small grains sizes, distorted and columnar structure as well as hydrogen contamination and defects induced by the process can explain such values. Films of lower thickness generally exhibit resistivity values ranging between 25 and 200  $\mu\Omega\text{cm}$  depending on the process.

## 7. Superconducting Properties

### 7.1. $\gamma\text{-Mo}_2\text{N}$ and $\beta\text{-Mo}_2\text{N}$ Phase

$\gamma\text{-Mo}_2\text{N}$  compounds exhibit superconducting transition at critical temperatures  $T_c$  as low as 4–5 K. Bull *et al.* [24] have synthesized the molybdenum nitride phase by high-pressure high-temperature process and have measured a  $T_c$  value of 5.2 K. The same value has been found by Inumaru *et al.* [33], who have deposited  $\beta\text{-Mo}_2\text{N}$  films by pulsed laser method.

In a recent work, Luo *et al.* [56] have studied the growth of epitaxial Mo<sub>2</sub>N films on SrTiO<sub>3</sub>. They report a  $T_c$  value of 4.5 K (Figure 5b).

Ihara *et al.* [25] have investigated the electronic structure and the superconducting transition temperature  $T_c$  of molybdenum nitride films deposited by reactive dc sputtering. The valence-band spectra change continuously from Mo to NaCl-B1-type cubic MoN<sub>1.8</sub> with increasing nitrogen concentration. The  $T_c$  of cubic Mo<sub>2</sub>N films is equal to 6–7 K with a wide transition width of 1–2 K.

Saito *et al.* [26] have reported a  $T_c$  of 4–5 K for  $\gamma$ -Mo<sub>2</sub>N films prepared from Mo thin films implanted with N ions.

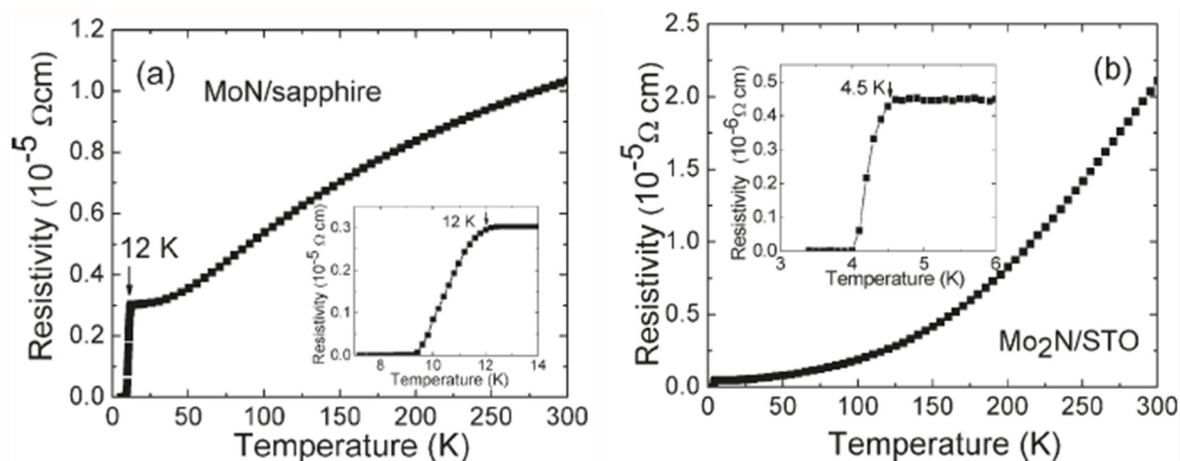


**Figure 5.** (a) Temperature dependence of resistivity of hexagonal MoN on Al<sub>2</sub>O<sub>3</sub>; and (b) temperature dependence of resistivity of hexagonal MoN on STO. The inset is the plot of resistivity at low temperature [56]. Copyright ACS Publications 2011.

As a general rule, the superconducting transition temperature is sensitive to the crystallinity, stoichiometry, and oxygen concentration.

### 7.2. $\delta$ -MoN Phase

The hexagonal MoN film exhibits a  $T_c$  value of 13.2 K with a transition width of 0.4 K [25]. A lower value equal to 4 K has been measured for hexagonal films made by ion implantation [26].

Luo *et al.* [56] have reported a  $T_c$  value equal to 12 K for hexagonal MoN epitaxially deposited on cut Al<sub>2</sub>O<sub>3</sub> (Figure 5a). A similar value has been determined for  $\delta_3$ -MoN (P6<sub>3</sub>mc, space group) by Ganin *et al.* [36]. Mo<sub>5</sub>N<sub>6</sub> is also superconducting with  $T_c$  equal to 12 K, whereas a lower value of 4 K has been determined for  $\delta_1$ -MoN (P6m2, space group). However, this value increases up to 6 K when the sample is heated at 923 K instead of 873 K.

### 7.3. Stoichiometric MoN Phase of Cubic Structure

The energy band structure of transition metal nitrides such as VN, MoN, CrN, NbN, *etc.* as well as the superconducting transition temperature has been extensively studied by Papaconstantopoulos *et al.* [42] by using the self-consistent semi-relativistic augmented-plane-wave (APW) method. Because of the high density of states (DOS) at the Fermi level and the high value of the electron–phonon interaction constant,

the superconducting transition temperature  $T_c$  values are rather high. NbN of NaCl-B1-type cubic structure exhibits a  $T_c$  value of 17 K. Since the addition of an extra electron moves the Fermi level into a region with considerably higher DOS, the  $T_c$  value corresponding to MoN of similar structure could be higher than 30 K. However, the attempts to synthesize well-ordered stoichiometric cubic MoN did not succeed. Transition metal nitrides form with a large concentration of vacancies on the nonmetal sublattice, and to a lesser extent on the metal sublattice that lower  $T_c$ . Moreover, the loss of long range order in sputtered films due to columnar growth may also reduce  $T_c$ .

The valence-band spectrum corresponding to the overstoichiometric cubic MoN<sub>1.5</sub> has a strong resemblance to the theoretical DOS calculated for the stoichiometric MoN phase of cubic structure, whereas the valence band spectrum of the stoichiometric MoN phase is not similar to the theoretical DOS [25]. Thus, the  $T_c$  value of B1-MoN films would decrease because of the vacancies and interstitial defects.

It is reported that high- $T_c$  refractory compounds like NbC and NbN are rather sensitive to disorder induced by ion irradiation [40]. The stoichiometric MoN films of cubic structure produced by reactive sputtering and ion implantation exhibit  $T_c$  values equal to 3 and 6 K, respectively. These results are consistent with those obtained in reference [26]. According to the authors, the low values of  $T_c$  may be due to the inhomogeneity of samples and the presence of radiation-induced point defects and radiation-induced disorder in the nitrogen and/or molybdenum sublattice in the B1 structure.  $T_c$  increases up to 6.8 K with increasing nitrogen dose up to  $5 \times 10^{17}$  ions cm<sup>-2</sup> in ion implantation process which corresponds to the transition from cubic  $\gamma$ -Mo<sub>2</sub>N to B1-MoN.

To our knowledge, the highest  $T_c$  value has been obtained by Savvides [41] who has deposited 400-nm-thick films by the low-energy ion-assisted method. The value corresponding to molybdenum nitride films processed at substrate temperature and ion energy of 773 K and 100 eV, respectively, increases from 6.2 K to 11.45 K after annealing at 973 K in a nitrogen ambient for 150 h. Annealing under such conditions allows the nitrogen concentration to be reduced from 56 at% to 48 at%.

In summary, the highest temperature  $T_c$  was obtained for amorphous  $\delta_3$ -MoN characterized by short Mo–Mo distances. The Mo<sub>5</sub>N<sub>6</sub> crystalline solid would have a high superconducting temperature value  $T_c$  but this characteristic could be due to the contamination by  $\delta_3$ -MoN phase because of the low diamagnetic response [36]. As previously seen, owing to nitrogen vacancies and radiation damages induced by non-equilibrium processes, the predicted high superconducting structure cannot be synthesized. Even if the valence band displays by MoN<sub>1.5</sub> is similar to the theoretical DOS corresponding to the stoichiometric B1-MoN phase [25], the superconducting temperature decreases from 12.5 to below 4.2 K with increasing x in MoN<sub>x</sub> structure from 1.1 to 1.8.

The low-energy ion-assisted method [41] could be able to synthesize such a structure with an annealing step conducted in pure N<sub>2</sub> gas at 973 K, which probably promotes the atoms ordering in the structure since the highest superconducting temperature has been achieved.

## 8. Some Other Properties

Owing to their very good catalytic properties, molybdenum nitrides are compared with noble metals. This is due to the presence of nitrogen atoms in interstitial sites of the host metal which modifies the density of states at the Fermi level. Thus, molybdenum nitrides are very active for adsorption and catalytic activities. Since the specific surface area is one of the most important characteristics of a good

catalyst, most experiments are made with nanosized powders, nanoporous materials, *etc.* However, because of the increasing interest in such properties for the future, we briefly present some recent works on the subject, keeping in mind that coatings could be promising for the future.

Tagliazucca *et al.* [19,20] have reported the influence of microstructure (nanocrystalline domains, porosity) on the catalytic activity of two molybdenum nitrides prepared by ammonolysis at temperatures of 923 and 1073 K. MoN-923 has higher conversion rates (3%–15%) during five reaction cycles in the 723–873 K range compared with MoN-1073 because MoN-923 displays smaller domain sizes and higher surface area. Moreover, the mechanical activation by ball milling of both samples reduces the domain sizes, narrows the distribution of the domain sizes, decreases the defects content, and then improves the catalytic activity during the first cycle considerably.

The good electronic conductivity as well as the moderately high surface area makes the molybdenum nitrides potential candidates for supercapacitors electrodes [61]. Nanostructured materials are especially interesting for such applications. MoN<sub>x</sub> powders ( $0.77 < x < 1.32$ ) with a crystallite size of 9 nm, a specific surface area of  $49 \text{ m}^2\text{g}^{-1}$  and an electrical conduction of  $7.51 \times 10^3 (\Omega\text{m})^{-1}$  display a specific capacitance value equal to  $111 \text{ Fg}^{-1}$  [61].

Among all catalyzed reactions, the hydrogen evolution reaction (HER) will have an increasing importance in the future because it is a carbon free alternative for hydrogen generation. This reaction is usually catalyzed by platinum, however less scarce and less expensive molybdenum nitrides as well as carbides are promising to replace platinum.

In a very recent work, Ma *et al.* [62] have synthesized  $\gamma$ -Mo<sub>2</sub>N nanoparticles (5–25 nm) and found that the overpotential needed to drive a current density of  $10 \text{ mAcm}^{-2}$  is equal to 353 mV. Nevertheless, this value remains higher than the one corresponding to  $\alpha$ -Mo<sub>2</sub>C, which is equal to 176 mV, *i.e.*, 100 mV higher than the value corresponding to platinum.

In another work, Chen *et al.* [63] have prepared carbon-supported molybdenum nitride nanoparticles  $\gamma$ -Mo<sub>2</sub>N-C (11 nm) and  $\delta$ -MoN-C (5 nm) as well as molybdenum carbide nitride composites from solid state reaction involving soybean powder and ammonium molybdate; the so-called MoSoy catalyst. This compound exhibits better characteristics than bulk platinum. The overpotential needed for driving a current density of  $10 \text{ mAcm}^{-2}$  is equal to 109 mV. Moreover, the catalyst is highly durable in a corrosive acidic solution over a period exceeding 500 h.

## 9. Conclusions

The unique combination of physical and chemical characteristics which is the result of the wide range of stoichiometry of molybdenum nitrides makes them very interesting and promising for various applications. The stable and nonstoichiometric  $\gamma$ -Mo<sub>2</sub>N<sub>1 ± x</sub> phase of NaCl-B1-type cubic structure exhibits good catalytic properties, whereas the stable and stoichiometric  $\delta$ -MoN phases of hexagonal structure have very high bulk moduli in the range of compressibility of c-BN and diamond, which make them potential candidates for ultra-incompressible and hard materials. The metastable and stoichiometric MoN phase of NaCl-B1-type cubic structure is a potential candidate for a high temperature superconductor. The critical temperature is the highest of all refractory carbides and nitrides and could be higher than 30 K. However, owing to the occurrence of point defects or disorder in the nitrogen and/or molybdenum sublattices in the B1 structure, the attempts to obtain high critical temperatures did not

succeed. Nanocrystalline and amorphous structures have also been obtained in a large range of stoichiometry. Molybdenum nitride films can be synthesized by various deposition processes from reactive sputtering to thermal decomposition of precursors. The composition and the structure of films as well as the chemical-physical properties depend on process parameters such as nitrogen pressure and dose, temperature and nature of substrate, composition of plasma, treatment duration, and also the occurrence of stresses during the film growth. These characteristics are correlated to the electronic structure and chemical bonding in molybdenum nitrides. Thus, an accurate control of the process parameters as well as a thorough study of electron states and chemical bonding by the band theory and quantum chemistry could lead to processes of new compounds and materials with an optimal combination of required properties.

### Acknowledgments

We gratefully acknowledge the Region Limousin for supporting the work on surface reactivity.

### Author Contributions

Isabelle Jauberteau drafted and organized this review article. Annie Bessaudou focused on the information about reactive sputtering methods, Richard Mayet, Julie Cornette, Jean Louis Jauberteau and Pierre Carles focused on the information about X-ray diffraction results, Raman spectroscopy results, plasma chemistry and structures of molybdenum nitride films, respectively. Thérèse Merle-Méjean reviewed the article.

### Conflicts of Interest

The authors declare no conflict of interest.

### References

1. Toth, L. *Transition Metal Carbides and Nitrides*; Academic Press: New York, NY, USA; London, UK, 1971; pp. 29, 247–261.
2. Oyama, S.T. Introduction to the chemistry of transition metal carbides and nitrides. In *The Chemistry of Transition Carbides and Nitrides*; Oyama, S.T., Ed.; Blackie Academic and Professional: London, Glasgow, UK, 1996; pp. 2–10.
3. Gubanov, V.A.; Ivanovsky, A.L.; Zhukov, V.P. Electronic structure and interatomic interactions in transition-metal nitrides. In *Electronic Structure of Refractory Carbides and Nitrides*; Gubanov, V.A., Ivanovsky, A.L., Zhukov, V.P., Eds.; Cambridge University Press: Cambridge, UK, 1994; pp. 70–75.
4. Chen, W.; Jiang, J.Z. Elastic properties and electronic structures of 4d- and 5d-transition metal mononitrides. *J. Alloys Compd.* **2010**, *499*, 243–254.
5. Aouadi, S.M.; Paudel, Y.; Luster, B.; Stadler, S.; Kohli, P.; Muratore, C.; Hager, C.; Voevodin, A.A. Adaptive Mo<sub>2</sub>N/MoS<sub>2</sub>/Ag Tribological nanocomposite coatings for aerospace applications. *Tribol. Lett.* **2008**, *29*, 95–103.

6. Aouadi, S.M.; Paudel, Y.; Simonson, W.J.; Ge, Q.; Kohli, P.; Muratore, C.; Voevodin, A.A. Tribological investigations of adaptive Mo<sub>2</sub>N/MoS<sub>2</sub>/Ag coatings with high sulfur content. *Surf. Coat. Technol.* **2009**, *203*, 1304–1309.
7. Gulbinski, W.; Suszko, T. Thin films of Mo<sub>2</sub>N/Ag nanocomposite—the structure, mechanical and tribological properties. *Surf. Coat. Technol.* **2006**, *201*, 1469–1476.
8. Khojier, K.; Karami Mehr, M.R.; Savaloni, H. Annealing temperature effect on the mechanical and tribological properties of molybdenum nitride thin films. *J. Nanostruct. Chem.* **2013**, *3*, 1–7.
9. Kattelus, H.; Koskenala, J.; Nurmela, A.; Niskanen, A. Stress control of sputter-deposited Mo–N films for micromechanical applications. *Microelectron. Eng.* **2002**, *60*, 97–105.
10. Rische, D. MOCVD of Tungsten and Molybdenum Nitrides. Ph.D. Thesis, University of Bochum, Bochum, Germany, 2007.
11. Alen, P. Atomic Layer Deposition of TaN, NbN and MoN films for Cu Metallizations. Ph.D. Thesis, University of Helsinki, Helsinki, Finland, 2005.
12. Guntur, V. Molybdenum Nitride Films in the Back Contact Structure of Flexible Substrates CdTe Solar Cells. Ph.D. Thesis, University of South Florida, Tampa, USA, 2011.
13. Shuangxi, S.; Yuzhang, L.; Dali, M.; Huiqin, L.; Ming, L. Diffusion barrier performances of thin Mo, Mo–N and Mo/Mo–N films between Cu and Si. *Thin Solid Films* **2005**, *476*, 142–147.
14. Reid, J.S. MEMS with Flexible Portions Made of Novel Materials. U.S. Patent 7071520B2, 4 July 2006.
15. Nagai, M. Transition-metal nitrides for hydrotreating catalyst—synthesis, surface properties, and reactivities. *Appl. Catal. A Gen.* **2007**, *322*, 178–190.
16. McKay, D. Catalysis over Molybdenum Containing Nitride Materials. Ph.D. Thesis, University of Glasgow, Glasgow, UK, 2008.
17. Zhu, J.F.; Guo, J.C.; Zhai, R.S.; Bao, X.; Zhang, X.Y.; Zhuang, S. Preparation and adsorption properties of Mo<sub>2</sub>N model catalyst. *Appl. Surf. Sci.* **2000**, *161*, 86–93.
18. Shi, C.; Zhu, A.M.; Yang, X.F.; Au, C.T. On the catalytic nature of VN, Mo<sub>2</sub>N and W<sub>2</sub>N nitrides for NO reduction with hydrogen. *Appl. Catal. A Gen.* **2004**, *276*, 223–230.
19. Tagliazucca, V.; Schlichte, K.; Schüth, F.; Weidenthaler, C. Molybdenum-based catalysts for the decomposition of ammonia: *In situ* X-ray diffraction studies, microstructure, and catalytic properties. *J. Catal.* **2013**, *305*, 277–289.
20. Tagliazucca, V.; Leoni, M.; Weidenthaler, C. Crystal structure and microstructural changes of molybdenum nitrides traces during catalytic reaction by *in situ* X-ray diffraction studies. *Phys. Chem. Chem. Phys.* **2014**, *16*, 6182–6188.
21. Gong, S.W.; Chen, H.K.; Li, W.; Li, B.Q. Catalytic behaviors of β-Mo<sub>2</sub>N<sub>0.78</sub> as a hydrodesulfurization catalyst. *Energy Fuels* **2006**, *20*, 1372–1376.
22. Jehn, H.; Ettmayer, P. The molybdenum-nitrogen phase diagram. *J. Less-Common Met.* **1978**, *58*, 85–98.
23. Karam, R.; Ward, R. The Preparation of β-Molybdenum Nitride. *Inorg. Chem.* **1970**, *9*, 1385–1387.
24. Bull, C.L.; Kawashima, T.; McMillan, P.F.; Machon, D.; Shebanova, O.; Daisenberger, D.; Soignard, E.; Takayama-Muromachi, E.; Chapon, L.C. Crystal structure and high-pressure properties of γ-Mo<sub>2</sub>N determined by neutron powder diffraction and X-ray diffraction. *J. Solid State Chem.* **2006**, *179*, 1762–1767.

25. Ihara, H.; Kimura, Y.; Senzaki, K.; Zezuka, H.; Hirabayashi, M. Electronic structures of B1 MoN, fcc Mo<sub>2</sub>N and hexagonal MoN. *Phys. Rev. B* **1985**, *31*, 3177–3178.
26. Saito, K.; Asada, Y. Superconductivity and structural changes of nitrogen-ion implanted Mo thin films. *J. Phys. F Met. Phys.* **1987**, *17*, 2273–2283.
27. Wu, J.D.; Wu, C.Z.; Zhong, X.X.; Song, Z.M.; Li, F.M. Surface nitridation of transition metals by pulsed laser irradiation in gaseous nitrogen. *Surf. Coat. Technol.* **1997**, *96*, 330–336.
28. Mändl, S.; Manova, D.; Gerlach, J.W.; Assmann, W.; Neumann, H. Rauschenbach, B. High temperature nitrogen plasma immersion ion implantation into molybdenum. *Surf. Coat. Technol.* **2004**, *180–181*, 362–366.
29. Anitha, V.P.; Major, S.; Chandrashekhar, D.; Bhatnagar, M. Deposition of molybdenum nitride films by r.f. reactive magnetron sputtering. *Surf. Coat. Technol.* **1996**, *79*, 50–54.
30. Hones, P.; Martin, N.; Regula, M.; Lévy, F. Structural and mechanical properties of chromium nitride, molybdenum nitride, and tungsten nitride thin films. *J. Phys. D Appl. Phys.* **2003**, *36*, 1023–1029.
31. Wang, Y.; Lin, R.Y. Amorphous molybdenum nitride thin films prepared by reactive sputter deposition. *Mater. Sci. Eng. B* **2004**, *112*, 42–49.
32. Stöber, L.; Konrath, J.P.; Krivec, S.; Patocka, F.; Schwartz, S.; Bittner, A.; Schneider, M.; Schmid, U. Impact of sputter deposition parameters on molybdenum nitride thin films properties. *J. Micromech. Microeng.* **2015**, *25*, doi:10.1088/0960-1317/25/7/074001.
33. Inumaru, K.; Baba, K.; Yamanaka, S. Synthesis and Characterization of superconducting  $\beta$ -MoN crystalline phase on a Si substrate: An application of pulsed laser deposition to nitride chemistry. *Chem. Mater.* **2005**, *17*, 5935–5940.
34. Jauberteau, I.; Jauberteau, J.L.; Goudeau, P.; Soulestin, B.; Marteau, M.; Cahoreau, M.; Aubreton, J. Investigations on a nitriding process of molybdenum thin films exposed to (Ar–N<sub>2</sub>–H<sub>2</sub>) expanding microwave plasma. *Surf. Coat. Technol.* **2009**, *203*, 1127–1132.
35. Lowther, J.E. Lattice model for the properties of non-stoichiometric cubic and hexagonal molybdenum nitride. *J. Alloys Compd.* **2004**, *364*, 13–16.
36. Ganin, A.Y.; Kienle, L.; Vajenine, G.V. Synthesis and characterization of hexagonal molybdenum nitrides. *J. Solid State Chem.* **2006**, *179*, 2339–2348.
37. Bull, C.L.; McMillan, P.F.; Soignard, E.; Leinenweber, K. Determination of the crystal structure of  $\delta$ -MoN by neutron diffraction. *J. Solid State Chem.* **2004**, *177*, 1488–1492.
38. Kanoun, M.B.; Goumri-Said, S.; Jaouen, M. Structure and mechanical stability of molybdenum nitrides: A first-principles study. *Phys. Rev. B* **2007**, *76*, doi:10.1103/PhysRevB.76.134109.
39. Zhao, E.; Wang, J.; Wu, Z. Displacive phase transition, structural stability, and mechanical properties of the ultra-incompressible and hard MoN by first principles. *Phys. Status Solidi B* **2010**, *247*, 1207–1213.
40. Linker, G.; Smithey, R.; Meyer, O. Superconductivity in MoN films with NaCl structure. *J. Phys. F Met. Phys.* **1984**, *14*, L115–L119.
41. Savvides, N. High  $T_c$  superconducting B1 phase MoN films prepared by low-energy ion-assisted deposition. *J. Appl. Phys.* **1987**, *62*, 600–610.

42. Papaconstantopoulos, D.A.; Pickett, W.E.; Klein, B.M.; Boyer, L.L. Electronic properties of transition-metal nitrides: The group-V and group-VI nitrides VN, NbN, TaN, CrN, MoN, and WN. *Phys. Rev. B* **1985**, *31*, 752–761.
43. Fix, R.; Gordon, R.G.; Hoffman, D.M. Low-temperature atmospheric-pressure metal-organic chemical vapor deposition of molybdenum nitride thin films. *Thin Solid Films* **1996**, *288*, 116–119.
44. Maoujoud, M.; Jardinier-Offergeld, M.; Bouillon, F. Synthesis and characterization of thin-film molybdenum nitrides. *Appl. Surf. Sci.* **1993**, *64*, 81–89.
45. Lyutaya, M.D. Formation of nitrides of the group VI transition metals. *Powder Metall. Met. Ceram.* **1979**, *18*, 190–196.
46. McKay, D.; Hargreaves, J.S.J.; Rico, J.L.; Rivera, J.L.; Sun, X.-L. The influence of phase and morphology of molybdenum nitrides on ammonia synthesis activity and reduction characteristics. *J. Solid State Chem.* **2008**, *181*, 325–333.
47. Birtill, J.; Dickens, P.G. Thermochemistry of Hydrogen Molybdenum Bronze Phases  $H_xMoO_3$ . *J. Solid State Chem.* **1979**, *29*, 367–372.
48. Cardenas-Lizana, F.; Gomez-Quero, S.; Perret, N.; Kiwi-Minsker, L.; Keane, M.A.  $\beta$ -Molybdenum nitride: Synthesis mechanism and catalytic response in the gas phase hydrogenation of p-chloronitrobenzene. *Catal. Sci. Technol.* **2011**, *1*, 794–801.
49. Thornton, J.A. High rate thick film growth. *Annu. Rev. Mater. Sci.* **1977**, *7*, 239–260.
50. Perry, A.J.; Baouchi, A.W.; Petersen, J.H.; Pozder, S.D. Crystal structure of molybdenum nitride films made by reactive cathodic arc evaporation. *Surf. Coat. Technol.* **1992**, *54/55*, 261–265.
51. Mändl, S.; Gerlach, J.W.; Assmann, W.; Rauschenbach, B. Phase formation and diffusion after nitrogen PIII in molybdenum. *Surf. Coat. Technol.* **2003**, *174–175*, 1238–1242.
52. Mändl, S.; Gerlach, W.; Rauschenbach, B. Nitride formation in transition metals during high fluence-high temperature implantation. *Surf. Coat. Technol.* **2005**, *200*, 584–588.
53. Jauberteau, I.; Merle-Méjean, T.; Touimi, S.; Weber, S.; Bessaudou, A.; Passelergue, A.; Jauberteau, J.L.; Aubreton, J. Expanding microwave plasma process for thin molybdenum films nitriding: Nitrogen diffusion and structure investigations. *Surf. Coat. Technol.* **2011**, *205*, S271–S274.
54. Jauberteau, I.; Jauberteau, J.L.; Touimi, S.; Merle-Méjean, T.; Weber, S.; Bessaudou, A. A thermochemical process using expanding plasma for nitriding thin molybdenum films at low temperature. *Engineering* **2012**, *4*, 857–868.
55. Jauberteau, I.; Mayet, R.; Cornette, J.; Bessaudou, A.; Carles, P.; Jauberteau, J.L.; Merle-Méjean, T. A reduction-nitridation process of molybdenum films in expanding microwave plasma: Crystal structure of molybdenum nitrides. *Surf. Coat. Technol.* **2015**, *270*, 77–85.
56. Luo, H.; Zou, G.; Wang, H.; Lee, J.H.; Lin, Y.; Peng, H.; Lin, Q.; Deng, S.; Bauer, E.; McKleskey, T.M.; *et al.* Controlling crystal structure and oxidation state in molybdenum nitrides through epitaxial stabilization. *J. Phys. Chem. C* **2011**, *115*, 17880–17883.
57. Nagae, M.; Yoshio, T.; Takemoto, Y.; Takada, J. Microstructure of a molybdenum nitride layer formed by nitriding molybdenum metal. *J. Am. Ceram. Soc.* **2001**, *84*, 1175–1177.
58. Soignard, E.; McMillan, P.F.; Chaplin, T.D.; Farag, S.M.; Bull, C.L.; Somayazulu, M.S.; Leinenweber, K. High-Pressure synthesis and study of low-compressibility molybdenum nitride ( $MoN$  and  $MoN_{1-x}$  phases). *Phys. Rev. B* **2003**, *68*, doi:10.1103/PhysRevB.68.132101.

59. Sahu, B.R.; Kleinman, L. Theoretical study of structural and electronic properties of  $\delta$ -MoN. *Phys. Rev. B* **2004**, *70*, doi:10.1103/PhysRevB.70.073103.
60. Hart, G.L.W.; Klein, B.M. Phonon and elastic instabilities in MoC and MoN. *Phys. Rev. B* **2000**, *61*, 3151–3154.
61. Choi, D.; Kumta, P.N. Synthesis and characterization of nanostructured niobium and molybdenum nitrides by a two steps transition metal halide approach. *J. Am. Ceram. Soc.* **2011**, *94*, 2371–2378.
62. Ma, L.; Ting, L.R.L.; Molinari, V.; Giordano, C.; Yeo, B.S. Efficient hydrogen evolution catalyzed by molybdenum carbide and molybdenum nitride nanocatalysts synthesized via the urea glass route. *J. Mater. Chem. A* **2015**, *3*, 8361–8368.
63. Chen, W.F.; Muckerman, J.T.; Fujita, E. Recent developments in transition metal carbides and nitrides as hydrogen evolution electrocatalysts. *Chem. Commun.* **2013**, *49*, 8896–8909.

© 2015 by the authors; licensee MDPI, Basel, Switzerland. This article is an open access article distributed under the terms and conditions of the Creative Commons Attribution license (<http://creativecommons.org/licenses/by/4.0/>).